AN EVALUATION OF THE EFFECTS OF A RAPIDLY CHANGING MIOCENE CLIMATE ON THE GROWTH AND STABLE ISOTOPIC ECOLOGY OF THE SCALLOP *CHESAPECTEN NEFRENS*

by

CULLEN LAPOINTE

(Under the Direction of Sally E. Walker)

ABSTRACT

We know little about how organisms respond to rapid climate change, especially within a latitudinally-restricted region. In this study, longevity and growth of scallops representing the warm Middle Miocene Climatic Optimum (MMCO) and cooler post-Miocene Climatic Transition (MCT) suggest that rapid global cooling did not significantly affect growth of *Chesapecten nefrens* within the Calvert Cliffs of Maryland.

Oxygen stable isotopes of *C. nefrens* calcite indicate significantly lighter $\delta^{18}O_{calcite}$ of MMCO than MCT (difference in means: -0.21‰ with 95% CI: -0.31 to -0.11‰). Shell intervals with low $\delta^{18}O_{calcite}$ coincided with growth bands, indicating summer growth cessation in MMCO and MCT *C. nefrens*. Carbon stable isotopes did not exhibit seasonal cycles, although $\delta^{13}C_{calcite}$ suggests significantly lower mean primary productivity in the MMCO than MCT. Results suggest that annual growth combined with stable isotopic analysis of scallops provide excellent paleoenvironmental insight into a climatically complex middle Miocene.

INDEX WORDS: Middle Miocene climatic optimum; Miocene climate transition; stable isotopic ecology; growth rate; longevity; scallop; seasonality; *Chesapecten*

AN EVALUATION OF THE EFFECTS OF A RAPDILY CHANGING MIOCENE CLIMATE ON THE GROWTH AND STABLE ISOTOPIC ECOLOGY OF THE SCALLOP *CHESAPECTEN NEFRENS*

by

CULLEN LAPOINTE

B.S., St. Lawrence University, 2016

A Thesis Submitted to the Graduate Faculty of The University of Georgia in Partial Fulfillment of the Requirements for the Degree

MASTER OF SCIENCE

ATHENS, GEORGIA

2018

AN EVALUATION OF THE EFFECTS OF A RAPDILY CHANGING MIOCENE CLIMATE ON THE GROWTH AND STABLE ISOTOPIC ECOLOGY OF THE SCALLOP *CHESAPECTEN NEFRENS*

by

CULLEN LAPOINTE

Major Professor:	Sally E. Walker
Committee:	Suzanne E. Pilaar Birch
	L. Bruce Railsback

Electronic Version Approved:

Suzanne Barbour
Dean of the Graduate School
The University of Georgia
May 2018

ACKNOWLEDGMENTS

Many thanks to Dr. Sally E. Walker for her patience and guidance throughout the course of this study. Her remarkable enthusiasm and curiosity encouraged me through the past two years. Thanks to my committee member, Dr. L. Bruce Railsback whose generosity and willingness to share his knowledge and the finer points of isotopic sampling were hugely helpful to the success of this project. Thanks also to my committee member Dr. Suzanne E. Pilaar Birch for integral contributions to the completion of this thesis. I would also like to thank Dr. Steven Holland for his statistical guidance through every part of this research.

Thanks are also due to John Nance and Dr. Stephen Godfrey of the Paleontology Collections at the Calvert Marine Museum Paleontology for bringing me in the field to bed 19 and allowing me spend a week in the collections measuring *Chesapecten*. Thanks also to Mike Ellwood the 'Amateur Geologist', for showing me outcrops of the Scientist's Cliffs and adding beautiful specimens to my sample and personal collection. This research was supported in part by the Watts-Wheeler Fund of the University of Georgia.

I would also like to thank all those geology graduate students, past and present, who have made spending hours in a windowless basement enjoyable. Thanks also to all those who have helped welcome me to this new town.

Finally, a very special thanks to my family. They are a very special crowd whom I am lucky to have in my life. My passion for science started with them, and my ability to keep that passion alive through the past couple of years is due entirely to their care and support.

TABLE OF CONTENTS

Page

LIST OF TABLES

Page

LIST OF FIGURES

Page

CHAPTER I

INTRODUCTION

Purpose of Study

Paleoclimatic studies are important in furthering our understanding of Earth's climatic history as well as the responses of organisms to changing climates (Jones & Gould, 1999; Johnson et al., 2009; Schone & Gillikin, 2013). The middle Miocene is of particular interest to paleoclimatic studies because of the rapid Miocene climatic transition (MCT: 14.5–13.5 Ma; Flower & Kennett, 1994; Zachos, et al., 2001; Greenop et al., 2014). Before MCT cooling, during the Middle Miocene Climatic Optimum (MMCO: 17.5–15.5 Ma), seawater temperatures were estimated to be ~3 °C warmer than present (Billups & Schrag, 2002; Holburn et al., 2004; Greenop et al., 2014). Following the MCT, global temperatures had cooled as much as 4 °C (Zachos et al., 2001). However, proposed temperature ranges and environmental conditions are poorly constrained for the time period, with most data originating from either deep-sea sediments or terrestrial records (Flower & Kennett, 1994; Zachos et al., 2001; Billups & Schrag, 2002; Holburn et al., 2004; Greenop et al., 2014). Very little climatic data exists for shallow marine environments of pre- and post-MCT conditions. An expansion of tropical species during the MMCO and turnover of marine species during the MCT suggest an organismal response to climate change (Zachos et al., 2001; Bohme, 2003; Holburn et al., 2004; Hayward et al., 2007; Greenop et al., 2014), yet little research has been done on this time period. Higher resolution climatic and organismal data is needed from additional environments to fully understand the effects of this rapidly changing climate.

Scallops are an ideal proxy to estimate in situ high resolution responses of organisms and their environments to changing climates (Krantz et al., 1984; Jones & Gould, 1999; Chauvaud et al., 2012; Chute et al., 2012). Scallop shells have high preservation potential and are present in a wide variety of marine environments and depth ranges since the middle Triassic (Waller, 2006). Scallops record climatic changes in two ways: shell growth and stable isotopic composition of shell calcite. Importantly, modern and fossil scallop studies have clarified the positive relationship between seawater temperature and scallop growth and longevity. Warmer temperatures promote higher growth rates and lower longevity, while colder temperatures yield lower growth rates and higher longevities (Krantz et al., 1984; Black et al., 1993; Chauvaud et al., 2012; Chute et al., 2012; Moss et al., 2016). Scallop growth is controlled secondarily by environmental primary productivity (Black et al., 1993; Chauvaud et al., 2012; Chute et al., 2012; Moss et al., 2016).

Shell calcite of scallops is accreted in isotopic equilibrium with the surrounding seawater (Krantz et al., 1987; Chauvaud et al., 1998; Goewert & Surge, 2008; Johnson et al., 2009; Goewert., 2010; Chauvaud et al., 2012). Shell growth may thus provide a weekly-to-monthly archive of $\delta^{18}O_{calcite}$ yielding seasonal temperature ranges and $\delta^{13}C_{calcite}$ approximating environmental primary productivity (Chauvaud et al., 1998; Goewert & Surge, 2008; Johnson et al., 2009; Chauvaud et al., 2012). Oxygen and carbon stable-isotopic profiles of shell calcite can establish high-resolution environmental conditions in which the scallops lived and whether their growth was affected by differences in temperature. While growth, longevity and stable isotopic analyses of scallops have been conducted in laboratory experiments or along latitudinal gradients, there is a need to study scallops living within a geographic locality to understand their in situ response to a changing climate.

My study evaluates the effects of a rapidly changing Miocene climate on growth parameters (longevity and growth rate) and isotopic ecology ($\delta^{18}O_{calcite}$ and $\delta^{13}C_{calcite}$) of *Chesapecten nefrens* from the Calvert Cliffs of Maryland. Longevity was predicted to increase from MMCO to MCT scallops, while growth rate was expected to decrease. Average $\delta^{18}O_{calcite}$ of MMCO *C. nefrens* was expected to be more negative than $\delta^{18}O_{calcite}$ of MCT *C. nefrens*. Seasonal extremes in $\delta^{18}O_{calcite}$ were used to determine timing of annuli formation. Carbon stable isotopes of MMCO shell calcite were predicted to be enriched in heavy carbon with the opposite predicted for MCT scallops. Cyclicity of $\delta^{13}C$ is expected to be lesser in MMCO scallops reflecting a more stable productivity level in the tropical environment. Shell growth and environmental reconstruction together make this the first comprehensive study of MCT climate change and the corresponding effect on mollusc autecology in the shallow-marine environment of the North-West Atlantic shelf.

An Overview of *Chesapecten nefrens*

Scallops (order Pectinidae) occur in the fossil record as early as the middle Triassic (Waller, 2006). Since then, their shells have been preserved in many marine environments from the deep-sea to shallow sub-tidal and from the poles to the tropics (Schöne & Surge 2005; Waller, 2006). Ward and Blackwelder (1975) introduced the scallop genus *Chesapecten* to include seven (now nine) species of large, ribbed, suspension-feeding bivalves. The genus first appeared in the early Miocene and went extinct during the late Pliocene. Adults grew up to 160 mm, but generally were about 100 mm; juveniles had maximum heights less than 20–30 mm (Ward & Blackwelder, 1975; Scalfani, 2011).

The genus *Chesapecten* dominated sections of dense shell beds of the Calvert Cliffs and ocurred in sandy shell-hash to fully articulated life positions (Kidwell, 1989; Verteuil & Norris, 1996; Vogt & Parrish, 2012). *Chesapecten* are used as stratigraphic indicators in the Calvert Cliffs as each species typically corresponds with a single formation (Scalfani, 2011). The species *Chesapecten nefrens* is the exception, occupying both the Calvert and Choptank Formations (Scalfani, 2011), which encompass the MCT.

Background and Literature Review

Longevity and Growth of Scallops. – Longevity and growth rates of marine organisms change with latitude and temperature, with decreasing temperatures inciting decreased metabolic rates (Doney et al., 2011; Chauvaud et al., 2012; Moss et al., 2016). Studies show temperature as the primary factor controlling variation of growth rates in modern scallops (Merrill et al., 1961; Chauvaud et al., 1998; Jones & Gould 1999; Goewert & Surge, 2008). One field study cites bottom-water temperatures as explaining greater than 76% of variation in scallop growth rates, with cooler waters leading to slower growth (Chauvaud et al., 1998). Reproductive cycles, chlorophyll and irradiance also explain growth variation in populations where temperature is not the main control (MacDonald & Thompson, 1988; Chauvaud et al., 1998; Chauvaud et al., 2012).

Modern studies show scallops accrete an annual growth band in response to growth cessation during seasonal temperature extremes or periods of reproduction (Merrill et al., 1965; Chauvaud et al., 1998; Hart & Chute, 2009). Annual bands (annuli) form predictably and so, a count of annuli yields a longevity estimate and measurements of annuli heights yield growth rates (Krantz et al., 1984; Hart & Chute, 2009). Paleontologic studies identified annuli on fossil

scallops to differing degrees of success (Krantz et al., 1984; Jones & Gould, 1999; Goewert & Surge 2008; Goewert, 2010). Fossil studies compared scallop longevity and growth along latitudinal gradients but have not explored the effect of temperature on longevity and growth within a single site.

Depending on their geographic range, scallops may accrete either summer or winter growth lines, or accrete annual bands in response to seasonal reproduction (Goewert, 2010; Chauvaud et al., 2012; Chute et al., 2012). The season of growth cessation is determined by comparing heights of observed annuli to seasonal cycles in oxygen stable isotopes of scallop calcite. Goewert (2010) studied growth and isotopic ecology of MMCO and middle Pliocene Warm Interval (MPWI) *Chesapecten* along a latitudinal gradient. Goewert (2010) concluded annual bands formed only in *Chesapecten* from the cooler MPWI period, and not in the Delaware or Florida MMCO samples.

Debates regarding the reliability of both annual growth rates as indicators of temperature change still abound. This study will evaluate longevity and growth of the scallop *Chesapecten nefrens* from two climatically-different, but geographically-consistent stratigraphic zones of the Calvert Cliffs to determine the effects of the changing Miocene climate on scallop longevity and growth.

$\delta^{18}O$ of Modern and Fossil Scallops. – Oxygen isotopes of molluscs are used in modern and fossil studies to approximate variation in seawater temperature (Emiliani, 1966; Jones & Allmon, 1995; Krantz et al., 1984; Owen et al., 2002; Chauvaud et al., 2005; Goewert & Surge, 2008; Johnson et al., 2009; Goewert 2010; Chauvaud et a., 2011; Chute et al., 2012). Stable isotopes incorporated into calcitic shell material are in relative isotopic equilibrium with the surrounding

seawater for most foraminifera and mollusc species, including many scallop species (Emiliani, 1966; Krantz et al., 1984; Jones & Allmon, 1995; Owen et al., 2002; Ravelo & Marcel, 2007; Johnson et al., 2009; Goewert 2010; Chauvaud et a., 2011; Chute et al., 2012). Oxygen isotopes are of particular interest to paleoclimate studies because $\delta^{18}O$ of scallop calcite ($\delta^{18}O_{calcite}$) is primarily controlled by water-column mixing, salinity and temperature (Chauvaud et al., 2005; Harris & Stokesbury, 2006; Ravelo & Marcel, 2007; Chute et al., 2012).

Global levels of $\delta^{18}O$ seawater ($\delta^{18}O_{seawater}$) are glacially dominated through the Miocene (Zachos et al., 2001; Goewert, 2010; Greenop et al., 2014). Fluvial input to the Calvert Cliffs during deposition of sampled intervals was minimal or absent, and likely did not influence levels of $\delta^{18}O_{calcite}$ (Browning et al., 2006; Vogt & Parrish, 2012; Kidwell et al., 2015). Evaporation and precipitation driven salinity changes are principally limited to the surface water (Ravelo & Marcel, 2007). Scallop biology and stratigraphy suggest that *Chesapecten nefrens* of the Calvert Cliffs reside in subtidal, open-shelf environments without fluvial input (Ward & Blackwelder 1975; Scalfani, 2011; Vogt & Parrish, 2012; Kidwell et al., 2015). With salinity eliminated as a likely cause of changing $\delta^{18}O_{seawater}$, my interpretations assumed temperature as the driving force of variation in $\delta^{18}O_{calcite}$.

Previous studies involving isotopic ecology of middle Miocene bivalves are minimal. Goewert (2010) evaluated the growth and isotopic ecology of *Chesapecten* from the MMCO. $\delta^{18}O_{calcite}$ of these *Chesapecten* lacked seasonal cycles, corroborating the lack of annual bands identified during growth analysis. Goewert attributed the lack of seasonal temperature variation to upwelling and coastal currents. Temperature reconstructions by Goewert (2010) calculated Delaware temperatures from shell calcite yielding a mean of 27±2.4°C ($n_{calcite}$=152), ranging

from 19.7 to 31.2°C (assumed $\delta^{18}O_{seawater}$: -0.35). Seawater temperatures of tropical marine environments today are 21 to 28°C (Goewert, 2010). Temperature estimates of Goewert (2010) place MMCO Delaware in the upper realm of tropical marine temperature ranges.

$\delta^{38}C$ of Modern and Fossil Scallops. – Studies of isotopic ecology of foraminifera and molluscs use $\delta^{13}C$ of shell calcite ($\delta^{13}C_{calcite}$) to estimate levels of surface primary productivity. The composition of $\delta^{13}C$ in shell calcite is accreted in relative equilibrium with $\delta^{13}C$ of environmental dissolved inorganic carbon ($\delta^{13}C_{DIC}$). Regionally, $\delta^{13}C_{DIC}$ reflects the carbon reservoir that is storing or releasing carbon. Carbon released from the lithosphere, most notably through volcanism, increases global $\delta^{13}C_{DIC}$ (Ravelo & Marcel, 2007; Diester-Haas et al., 2009). Photosynthesis preferentially takes up ^{12}C, leaving the terrestrial biosphere to accumulate depleted carbon stores (Ravelo & Marcel, 2007; Diester-Haas et al., 2009; Greenop et al., 2014). As terrestrial biosphere volume grows, global $\delta^{13}C_{DIC}$ increases. The middle Miocene was a time of maximum atmospheric $\delta^{13}C$ and a clear explanation of such high $\delta^{13}C$ levels is contested; likely a combination of volcanic activity and increased continental organic carbon reservoir are responsible for Miocene $\delta^{13}C$ excursion (Zachos et al., 1993; Diester-Haas et al., 2009; Greenop et al., 2014).

In marine environments, local changes in $\delta^{13}C_{DIC}$ are driven by respiration and photosynthesis and regionally by upwelling and advection. Mixing of surface to bottom waters also influences $\delta^{13}C_{calcite}$ of the benthic scallop (Ravelo & Marcel, 2007). As stated earlier, photosynthesis increases $\delta^{13}C_{DIC}$, but respiration reverses this process by releasing lighter carbon isotopes. An ontogenic trend of depletion as well as seasonal cycles have been observed in $\delta^{13}C$ of scallop shell calcite (Chauvaud et al., 2011).

CHAPTER II

METHODS

Study Site

Chesapecten nefrens valves were collected from slumped blocks below exposed shell beds 14 and 19 from Calvert Cliffs of Maryland (**Fig. 2.1**; 38° 24' N, 78° 24'), and supplemented by valves housed at the Calvert Marine Museum. Depositional zones of the Calvert Cliffs include four major shell beds (Kidwell, 1989). Shell beds are composed of dense shell material including fragmented to intact, and frequently articulated, *Chesapecten nefrens* valves. Major shell beds, including 14 and 19, are condensed, time-averaged transgressive deposits that accumulated over 100 k.y. time scales (**Fig. 2.2;** Kidwell, 1989; Browning et al., 2006; Vogt & Parrish, 2012).

Shell beds were deposited in open-shelf environments, with bed 14 lithology identified between inner shelf and shore-face, and bed 19 lithology identified from inner shelf to intertidal (Kidwell, 1989; Vogt & Parrish, 2012; Kidwell et al., 2015). Stratigraphy, biostratigraphy, and strontium chemostratigraphic dating placed deposition of shell bed 14 just after the peak MMCO, and bed 19 just after MCT (**Fig. 2.2**; Browning et al., 2006; Vogt & Parrish, 2012; Kidwell et al., 2015). The extent of cooling over the MCT is contested, with estimates ranging from 3 °C of deep-sea cooling (Zachos et al., 2001) to a more extreme estimate of 7 °C decrease in mean annual temperatures of coastal environments (Bohme, 2003).

Longevity and Growth Analysis

Only bottom valves were used in this study because they often lacked encrusting and bio-eroding organisms. For growth analysis, shells ≥ 90 mm in shell height (umbo to growing edge; **Fig. 2.3**) were chosen to ensure that enough annual growth lines were counted for the von Bertalanffy growth function (discussed below). Annual bands were assumed to represent a single year of growth for longevity and growth analyses. Of shells sampled, 26 were randomly selected from shell bed 14 (shell height: $\bar{x}$ =114.58 mm, sd=11.84) and 28 were randomly selected from bed 19 (shell height: $\bar{x}$ =115.99 mm, sd=15.69), for a total of 54 shells.

Recognizing Annuli and Shocklines. – Annuli are recognized as prominent, raised growth bands that extend, uninterrupted, across the width of the entire shell (**Fig. 2.3**; Merrill et al., 1965; Krantz et al., 1984; Hart & Chute, 2009). Visual assessment of annual bands is a commonly used method to age scallops (Johnson et al., 2009; Hart & Chute, 2009; Chauvaud et al., 2012; Chute et al., 2012). Shocklines can also occur on the shell, resulting from short-lived environmental disturbances (**Fig. 2.3;** Merrill et al., 1965; Krantz et al., 1984). Shocklines can be distinguished from annuli because they do not have stacked growth. Annuli were used to evaluate longevity and growth, while shocklines were used to examine environmental disturbance between the MMCO and MCT.

Longevity estimates. – A count of all annuli present on individual valves was used to determine scallop age (**Fig. 2.3**). Age estimates were also verified with resilifer growth lines (Merrill et al., 1965). A Mann-Whitney U-test was used to quantify differences between MMCO and MCT ages (R Core Team, 2017).

Shockline Abundance. – The abundance of shocklines on each shell was used to estimate the incidence of environmental disturbances between MMCO and MCT scallops. A Mann-Whitney U-Test (R Core Team, 2017) was used to determine if shockline abundance was significantly different between the MMCO and MCT scallop samples.

Growth Rate. – Shell growth rate declines exponentially throughout ontogenesis, and therefore, the non-linear von Bertalanffy growth function was used to calculate a constant (*K*) that described shell growth. The von Bertalanffy function required heights of successive annuli (H_t) to calculate growth parameters. Annuli heights were measured with electronic calipers to the nearest 0.01 mm (accuracy ±0.03 mm) between umbo and annuli for all 54 samples (**Fig. 2.3**). The von Bertalanffy equation has five major parameters:

$$H_t = \boldsymbol{L}_\infty * (1 - e^{\boldsymbol{K}(t - \boldsymbol{t_0})})$$

where both measured heights of each annulus (H_t in mm), and the age of the scallop at each identified annuli (t) are input from measurements of *C. nefrens* samples. The von Bertalanffy equation involves three growth constants: 1) *asymptotic height* ($\boldsymbol{L}_\infty$), which is the hypothetical maximum length an individual can reach; 2) the *Brody growth rate coefficient* (***K***), a constant that describes nonlinear growth-rate; and 3) *time-zero* ($\boldsymbol{t_0}$), an offset that enables the model to describe growth of the entire life span. This study focuses on the Brody growth coefficient (***K***) to approximate scallop growth rates using the von Bertalanffy growth function.

Because growth constants ($\boldsymbol{L}_\infty$, ***K***, and $\boldsymbol{t_0}$) are highly variable between individual scallops, models were generated, using the fishR package (Ogle, 2017; R Core Team, 2017). Models were used to determine if climatic change significantly affected the amount of explained variation in

measured annuli heights. The best-fit model was chosen based on the Akaike Information Criterion (AIC) determined using maximum likelihood analysis. The lowest AIC value indicated the 'best-fit' model. Confidence intervals of best-fit growth parameters determined if significant variability was present in growth between MMCO and MCT scallops.

To further compare growth of MMCO and MCT, the von Bertalanffy growth function was fitted to annuli heights of all scallop individuals. Growth rates (K) calculated for individuals were compared using a Welch two-sample t-test (R Core Team, 2017) to test for statistically significant differences in individual growth rates between MMCO and MCT samples.

Stable Isotopic Analysis

The isotopic ecology of two individual scallops from each bed was evaluated to determine if the scallops experienced seasonal temperature or productivity cycles. Stable isotopes were also used to quantify difference in environmental conditions experienced by MMCO and MCT scallops. Shells for isotopic analysis were chosen based on preservation of the valve (i.e. no substantial cracks, post-mortem drilling, or abrasion to outer layer).

Original calcitic composition of the shells. – Prior to isotopic analysis, the scallops were tested for original-calcitic composition using both an X-Ray Diffractometer (XRD) and petrographic thin sections. For the XRD, one shell from each bed was sampled at four intervals parallel and adjacent to the axis of growth ($\bar{x}$ weight = 2.00 ± 1.12 mg) using a dremmel drill (1/4 mm burr).

The eight samples were analyzed individually using a BRUKER D8 Advance model XRD with Co Kα radiation operated at 40 mA and 35 kV (with a 0.01 step size, Ni β-filter and Lynx-eye® position sensitive detector) housed within the Geology Department at the University

of Georgia. Samples were scanned between 20° and 60° 2θ range with the sample rotating 360° every 30 seconds. Results of XRD indicated a calcitic, and not aragonitic, composition of external shell material (Appendix B: Fig. B.1).

To determine original calcite composition of the area drilled for isotopic analysis, petrographic thin sections of two bottom valves, one each from bed 14 and 19, were made at Vancouver Petrographics Ltd. (Vancouver, British Columbia, Canada). Thin sections were examined under polarized light at 10X with a Leitz Lab 12 PolS microscope. The outer foliated calcite layer was apparent in both thin sections as was the prismatic calcitic inner layer. Together, XRD and thin section examination indicated the shell layers (chiefly, the outer foliated layer) to be drilled for isotopic analysis consisted of original, unaltered, calcite.

Sampling. – Powdered calcite samples were collected from transects of two *Chesapecten nefrens* from each of the two beds, 14 and 19. Valves chosen for isotopic analysis were shells P3 and P7 from bed 14 (shell heights: 107.05 mm and 110.32 mm respectively), and shells S2 and S5 from shell bed 19 (shell heights: 102.97 and 138.73 mm respectively).

Shells were sampled at 1 mm intervals (using a dental drill with ¼ diameter burr) along the axis of growth. The first sample was started 10 mm from the hinge to the first identified annulus and taken every millimeter thereafter to the growing edge. Each sample of powdered calcite was weighed ($\bar{x}$ weight: 0.075 mg) using the Cubis® Sartorius precision balance at the Sedimentary Geochemistry Lab, Geology Department at the University of Georgia and stored in a 4.5 ml borosilicate exetainer. Replicate samples were taken at observed annuli to compare isotopic data. The powdered samples were analyzed using a GasBench Isotope Ratio Mass Spectrometer at the University of Alabama-Tuscaloosa Geological Science Stable Isotope Lab.

All isotopic data are reported relative to the Vienna Pee Dee Belemnite standard (VPDB) in per mil (‰). Ratios of $^{18}O/^{16}O$ and $^{13}C/^{12}C$ are expressed in delta notation [$\delta^{18}O$ or $\delta^{13}C = (R_{shell}-R_{standard})/R_{standard}$]. Isotopic ratios normalized to VPDB were plotted against shell height resulting in isotopic profiles for $\delta^{18}O$ and $\delta^{13}C$ throughout scallop growth.

$\delta^{18}O_{calcite}$ of Chesapecten nefrens. – Evidence of seasonality in shell stable isotope composition was defined by cyclic peaks and troughs in $\delta^{18}O_{calcite}$ along a shell transect. The lightest (more negative) intervals of $\delta^{18}O_{calcite}$ within each transect were identified as warmer summer months, while the heaviest (more positive) intervals of $\delta^{18}O_{calcite}$ within each transect were identified as colder winter months. The average summer $\delta^{18}O_{calcite}$ was calculated with the minimum $\delta^{18}O_{calcite}$ sample of each summer interval within a single transect. The winter $\delta^{18}O_{calcite}$ maximum was determined as the maximum $\delta^{18}O_{calcite}$ sample of each annual cycle. Winter maximums were averaged for each shell individually. The average difference in summer and winter $\delta^{18}O_{calcite}$ of each shell yielded average annual amplitudes of seasonal change for each shell.

Measured heights of annuli observed during growth analysis were compared to $\delta^{18}O_{calcite}$. Annuli should form at predictable points along the profile, likely at either the lightest (summer growth cessation) or heaviest (winter growth cessation) $\delta^{18}O_{calcite}$ stable isotopic values. Isotopic ecology of annuli formation was compared between climatic periods. Ages determined through oxygen isotopes were compared to those resolved through a count of observed annuli.

Estimates of $\delta^{18}O_{seawater}$ are not available for the North Atlantic at high enough resolution to resolve MMCO and MCT temperatures. Therefore, means of MMCO and MCT $\delta^{18}O_{calcite}$ were compared to determine if they reflect a relatively warmer MMCO than MCT. A Welch two-sample *t*-test determined a difference in MMCO $\delta^{18}O_{calcite}$ and MCT $\delta^{18}O_{calcite}$ means.

$\delta^{13}C_{calcite}$ of Chesapecten nefrens. – Modern and fossil studies of scallop stable isotopes conclude $\delta^{13}C_{calcite}$ is accreted in isotopic equilibrium with $\delta^{13}C_{seawater}$; however minor metabolic and ontogenic effects complicate signals of $\delta^{13}C_{calcite}$ (Goewert, 2010; Chauvaud et al., 2011). A Welch two-sample *t*-test (R Core Team, 2017) compared MMCO $\delta^{13}C$ to MCT $\delta^{13}C$ and determined if statistically significant differences in environmental primary-productivity were present between the beds.

Figure 2.1. Calvert Cliffs study area. The site is marked with a red dot, in Maryland, United States. Inset is shell bed 19, outcropping just south of Calvert Cliffs State Park, Lusby, Maryland (adapted from Google Maps).

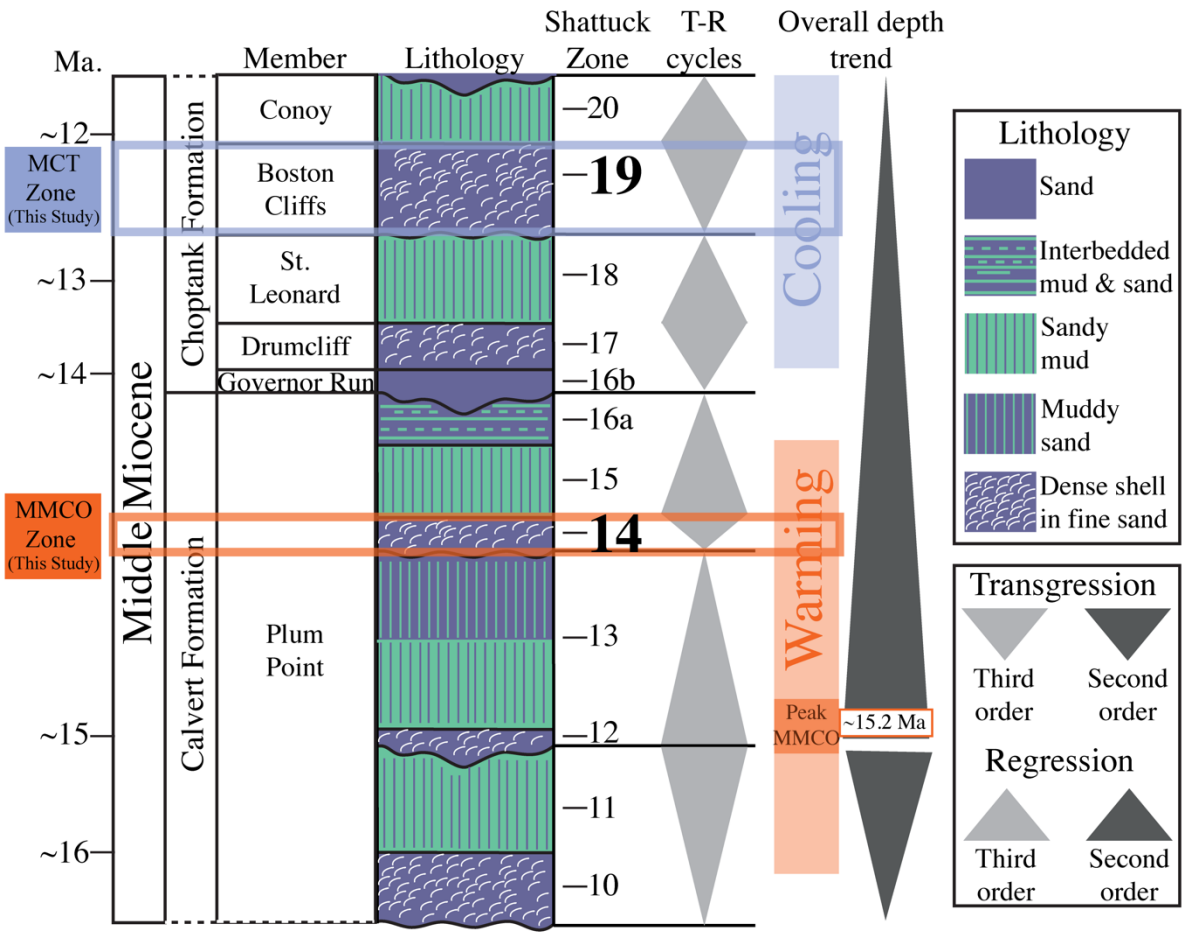

Figure 2.2. Stratigraphic column of the Calvert Cliffs study area. Lithology, transgression-regression cycles (T–R cycles) and climatic trends of middle Miocene Calvert Cliffs. I studied *Chesapecten nefrens* collected from bed 14 (MMCO), outlined in orange, and bed 19 (MCT), outlined in blue. Modified from Vogt & Parrish, 2012, and Kidwell et al., 2015.

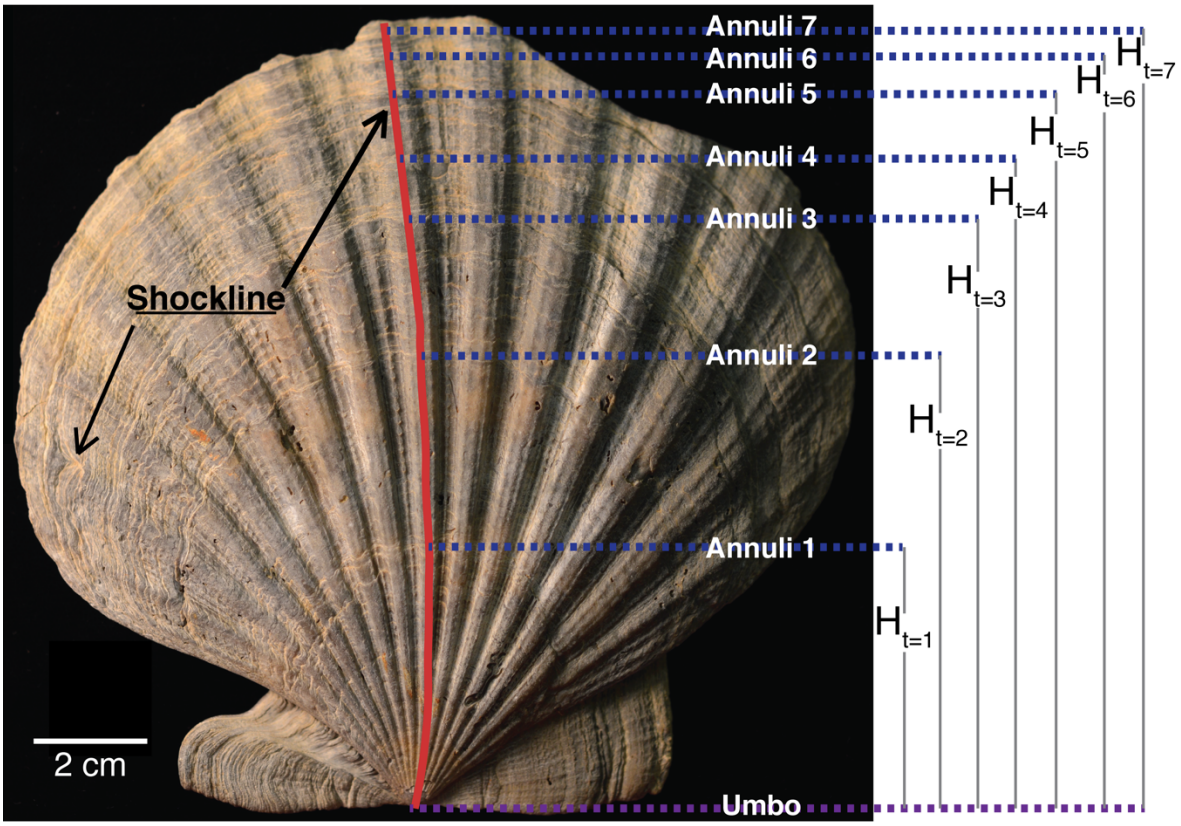

Figure 2.3. Bottom valve of *C. nefrens* showing annuli and measurements. Identified annuli are marked with dashed-blue lines along the axis of growth which is the red solid line. An arrow points out a shockline and probable evidence of corresponding predation. Based on annuli, this scallop is seven years old. H at time t is the height of each annulus, or the shell height at different years of growth.

CHAPTER III

LONGEVITY AND GROWTH RESULTS AND CONCLUSIONS

Results

*Longevity***. –** Longevity did not differ significantly between *Chesapecten nefrens* of warm and cool climatic regimes as we had expected (Mann-Whitney U-test of MMCO and MCT longevities: W=359.5, p=0.54). MMCO scallops and those of the MCT had similar longevities with means of 5.62 ± 1.7 yrs and 5.75 ± 1.82 yrs respectively (**Fig. 3.1**).

Distribution of longevities also appeared similar in MMCO and MCT scallops as 15 of 26 MMCO scallops and 16 of 28 MCT scallops had four annuli each (**Fig. 3.1**). The maximum age of a MMCO scallop was 11 yrs (height = 140.80 mm, shell M11; Appendix A, Table A.1) and the maximum age of a MCT scallop was 10 yrs (height =142.38 mm, shell C1; Appendix A, Table A.2). The largest shells from both beds, coincidentally, had eight annuli (MMCO max height=144.71 mm; MCT max height=157.22 mm). Overall longevity analysis of MMCO and MCT samples yielded similar results (**Fig. 3.1**).

Shockline Abundance. – A Wilcoxon rank sum test found insignificant differences between abundances of MMCO and MCT shocklines (MMCO shockline abundance: $\bar{x}$= 5.54; MCT shockline abundance: $\bar{x}$= 4.75; W=430, p= 0.251; Appendix A: Table A.1 & A.2).

*Growth***. –** Growth of *C. nefrens* was greater for MMCO than MCT, however, as the confidence intervals of $\boldsymbol{K}$ overlap, growth was not significantly different between the time periods ($\boldsymbol{K}_{\mathbf{MMCO}}$ =

0.33 with 95% CI: 0.29 to 0.37; $\boldsymbol{K}_{\mathbf{MCT}}$ = 0.31 with 95% CI: 0.27 to 0.34). The best-fit growth rates were identified using maximum likelihood analysis, with the lowest AIC score indicating the best-fit of a suite of models (model fit1LK; **Table 3.1; Fig. 3.2;** annuli heights Appendix A: Table A.3). A Welch two-sample *t*–test of growth rates calculated for individuals, also yielded insignificant differences between MMCO and MCT samples (MMCO *K*: $\bar{x}$= 0.39; MCT *K*: $\bar{x}$= 0.4; *t*=-0.075, df=51.52. p=0.945, Appendix A: Tables A.1 and A.2).

Discussion and Conclusion

Longevity was nearly similar between MMCO and MCT scallops. This disagrees with the majority of studies regarding the positive relationship between longevity and temperature. A minimum height requirement for sampled *C. nefrens* may have contributed to the similarity in MMCO and MCT annuli longevities, as the minimum age in both samples (four years) had the highest count (**Fig. 3.1**). The similarity in longevities between MMCO and MCT periods could be strongly influenced by the minimum height requirement of sampled *C. nefrens*. In addition to longevity, growth rates remained strikingly constant through the MMCO and MCT time periods (**Table 3.1; Fig. 3.2**). Similar longevities and growth could indicate a lesser change in temperature within the Calvert Cliffs than previously suggested for other middle Miocene environments, or, *Chesapecten nefrens* may have tracked preferred environments as cooling occurred with scallops either residing in cooler, deeper waters during warm periods or moving to warmer, shallower waters as cooling progressed. This would be apparent in the isotope record as oxygen isotopes would remain constant between bed 14 and bed 19 shells. A third possibility, is that annuli overestimated longevity and growth of the scallops. Observed annuli have resulted in

exaggerated longevities in previous fossil studies (Krantz et al., 1984; Goewert & Surge, 2008; Goewert, 2010). Annual cycles of $\delta^{18}O$ will provide a check of observed annuli counts and measurements.

Table 3.1. Akaike Information Criterion (AIC) of growth models. Parameters, L_∞ , K, and t_0 , were calculated using the von Bertalanffy equation in FishR. A [BED] label indicates a parameter that was calculated for each of the samples (MMCO and MCT). The lowest AIC score indicates fit1LK was the best-fit model to calculate K for MMCO and MCT populations. Fit1LK determined insignificant differences between K_{MMCO} (0.33 with 95% CI: 0.29 to 0.37) and K_{MCT} (0.31 with 95% CI: 0.27 to 0.34).

Model	Definition	df	AIC	K
fitGen	$H_t = L_\infty$ [BED] * (1-e $^{K\,[BED]\,(t - t_0\,[BED])}$)	7	2216.11	K_{MMCO}= 0.349 K_{MCT}= 0.294
fit1Kt_0	$H_t = L_\infty$ * (1-e $^{K\,[BED]\,(t - t_0\,[BED])}$)	6	2217.63	K_{MMCO}= 0.314 K_{MCT}= 0.322
fit1Lt_0	$H_t = L_\infty$ [BED] * (1-e $^{K\,(t - t_0\,[BED])}$)	6	2216.38	K_{ALL}= 0.319
fit1LK	$H_t = L_\infty$ [BED] * (1-e $^{K\,[BED]\,(t - t_0)}$)	6	2214.99	K_{MMCO}= 0.333 K_{MCT}= 0.308
fit2t_0	$H_t = L_\infty$ * (1-e $^{K\,(t - t_0\,[BED])}$)	5	2216.20	K_{ALL}= 0.318
fit2K	$H_t = L_\infty$ * (1-e $^{K\,[BED]\,(t - t_0)}$)	5	2215.74	K_{MMCO}= 0.315 K_{MCT}= 0.321
fit2L	$H_t = L_\infty$ [BED] * (1-e $^{K\,(t - t\,)}$)	5	2214.62	K_{ALL}= 0.319
fitCom	$H_t = L_\infty$ * (1-e $^{K\,(t - t_0)}$)	4	2214.46	K_{ALL}=0.319

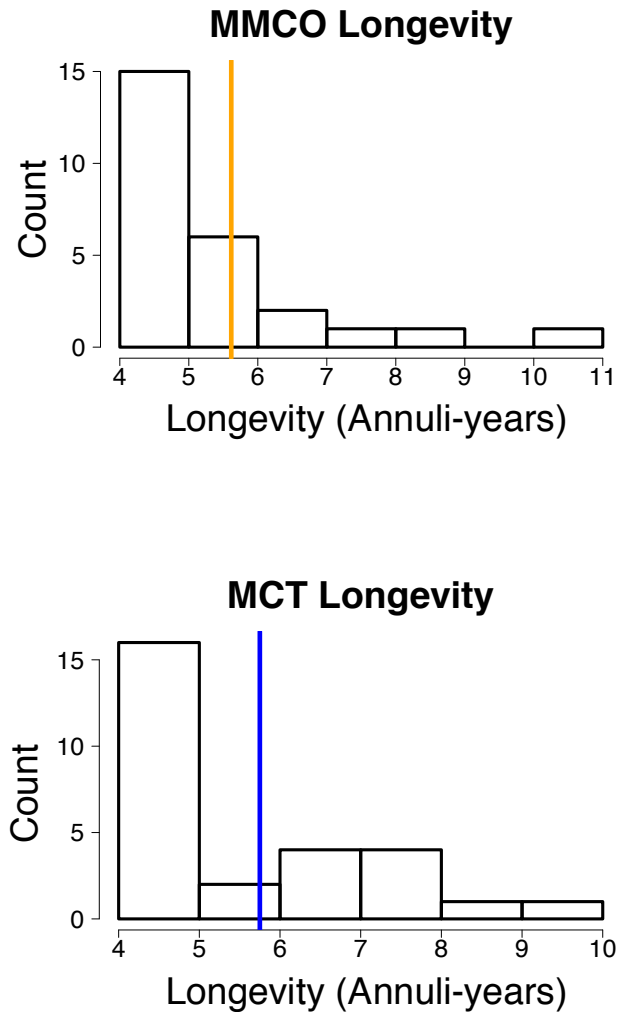

Figure 3.1. Longevity histograms for MMCO and MCT *C. nefrens*. Sample size for MMCO is 26 scallops and 28 scallops for MCT. The mean longevity for each bed is marked by a vertical line (MMCO [orange line]: 5.62 ± 1.7 yrs; MCT [blue line]: 5.75 ± 1.82 yrs). Scallops sampled for isotopic analysis were five years old for MMCO and 4 & 7 for MCT. Data in Appendix A: Tables A.1 and A.2.

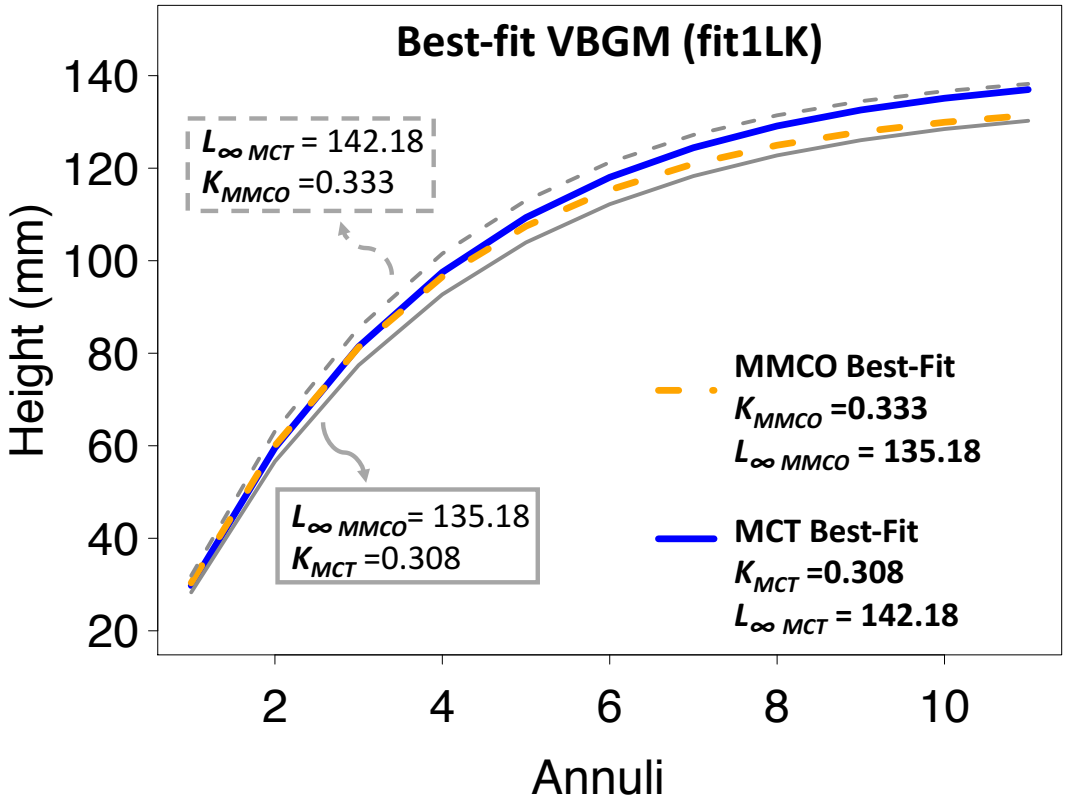

Figure 3.2. von Bertalanffy growth model for *C. nefrens*. The best-fit von Bertalanffy growth model (VBGM) producing MMCO and MCT ***K*** estimates is fit1LK. MMCO growth (yellow dashed line) is faster than MCT (solid blue line), but the difference is not statistically significant ($\boldsymbol{K_{MMCO}}$ = 0.33 with 95% CI: 0.29 to 0.37; $\boldsymbol{K_{MCT}}$ = 0.31 with 95% CI: 0.27 to 0.34). Asymptotic height (L_∞) was less in MMCO than MCT, but again the difference does not differ significantly ($\mathbf{L_{\infty MMCO}}$ = 135.18 mm with 95% CI: 128.49 to 141.87; $\mathbf{L_{\infty MCT}}$ = 142.18 mm with 95% CI: 135.11 to 149.25). Gray solid line shows $\boldsymbol{K_{MCT}}$ relative to the $\mathbf{L_{\infty MMCO}}$ estimate. Gray dashed line shows $\boldsymbol{K_{MMCO}}$ relative to the $\mathbf{L_{\infty MCT}}$ estimate.

CHAPTER IV

STABLE ISOTOPIC RESULTS AND CONCLUSIONS

Results

$\delta^{18}O_{calcite}$ of Chesapecten nefrens. – Both MMCO and MCT profiles displayed seasonality of $\delta^{18}O_{calcite}$ and the range of MMCO $\delta^{18}O_{calcite}$ (–1.3 to 1.4 ‰; **Figs. 4.1 & 4.2**) was less than MCT $\delta^{18}O_{calcite}$ (–1.35 to 2.00 ‰; **Figs. 4.1 & 4.3**). MMCO shell P3 had a mean $\delta^{18}O_{calcite}$ of 0.15‰ (the range of P3 $\delta^{18}O_{calcite}$ was –1.3 to 1.4‰; **Fig. 4.2A**). MMCO shell P7 $\delta^{18}O_{calcite}$ had a mean of 1.77‰ (the range of P7 $\delta^{18}O_{calcite}$ was –1.1 to 1.2 ‰; **Fig. 4.2B**). Mean $\delta^{18}O_{calcite}$ of MCT shell S2 was 0.34 ‰ (the range of S2 $\delta^{18}O_{calcite}$ is –1.35 to 1.77 ‰; **Fig. 4.3A**). MCT shell S5 had a mean $\delta^{18}O_{calcite}$ of 0.46‰ (the range of S5 $\delta^{18}O_{calcite}$ is –0.9 to 2.0‰; **Fig. 4.3B**).

MMCO scallops (P3 and P7) and MCT scallops (S2 and S5) both yielded greater annuli ages than $\delta^{18}O_{calcite}$ ages. MMCO $\delta^{18}O_{calcite}$ yielded three years of age, with growth cessation in summer months, while annuli yielded five years of age in MMCO scallops (**Table 4.1; Fig. 4.2**). However, annuli of MCT shell S2 corresponded exactly with $\delta^{18}O_{calcite}$ longevity with both methods yielding four years (**Table 4.1; Fig. 4.3A**). MCT shell S5 had five annuli, but only three $\delta^{18}O_{calcite}$ cycles (**Table 4.1; Fig. 4.3B**). MCT $\delta^{18}O_{calcite}$ indicated growth cessation in summer months.

The oxygen stable isotopic data indicates more extreme summer $\delta^{18}O_{calcite}$ minimums and less extreme winter $\delta^{18}O_{calcite}$ maximums in MMCO than MCT (**Table 4.2**). The mean of all six MMCO summer $\delta^{18}O_{calcite}$ minima is -1.08 ± 0.23‰. The mean of all seven MCT $\delta^{18}O_{calcite}$

summer minima was -0.73 ± 0.45‰. The mean of all eight MMCO winter $\delta^{18}O_{calcite}$ maxima was 1.09 ± 0.16‰. The mean of all seven winter $\delta^{18}O_{calcite}$ maxima for MCT scallops was 1.51 ± 0.30‰.

Observed annuli predicted summer growth cessation less accurately in MMCO *C. nefrens* than MCT. Observed annuli corresponded with only four of six MMCO $\delta^{18}O_{calcite}$ troughs (**Fig. 4.2**). However, those MMCO $\delta^{18}O_{calcite}$ troughs that did not align with observed annuli did align with observed shocklines. Observed annuli corresponded with all seven MCT $\delta^{18}O_{calcite}$ troughs (**Fig. 4.3A**). Growth bands coincident with troughs of $\delta^{18}O_{calcite}$ indicated summer growth cessation in both MMCO and MCT scallops.

The $\delta^{18}O_{calcite}$ was significantly lighter in MMCO scallops (mean = 0.16‰) than MCT (mean = 0.4‰; t = -3.45, df = 358.38, p = 0.0006; **Fig. 4.1**). A Welch two-sample t-test of MMCO and MCT of $\delta^{18}O_{calcite}$ yielded a difference in means of -0.27‰ (95% CI: -0.37 to -0.10 ‰).

$\delta^{13}C_{calcite}$ of Chesapecten nefrens. – The $\delta^{13}C_{calcite}$ was significantly lighter in MMCO *C. nefrens* than MCT, but variation of $\delta^{13}C_{calcite}$ did not appear to follow a seasonal cycle in either MMCO or MCT transects (**Figs. 4.2 & 4.3**). Distribution of shell carbon had a lower amplitude than oxygen (**Figs. 4.1 & 4.4**). Carbon isotope ratios varied significantly within MMCO and MCT shell material (t=–4.20, df=260.59, p=0.00004; **Fig. 4.4)**. The means of MMCO and MCT $\delta^{13}C_{calcite}$ had a difference of –0.21‰ (95% CI: -0.31 to -0.11‰; **Fig. 4.3**).

Discussion and Conclusion

$\delta^{18}O$ of Chesapecten nefrens. – Seasonality in $\delta^{18}O_{calcite}$ contradicts previous work of Goewert (2010) where no seasonality was present in MMCO *Chesapecten*. However, $\delta^{18}O_{calcite}$ of this study had the first trough at around 60 or 70 mm, so I suggest that Goewert (2010) had not sampled enough shell length to see seasonal cycles. The $\delta^{18}O_{calcite}$ of *C. nefrens* supports glaciation, with lighter MMCO than MCT $\delta^{18}O_{calcite}$, although the lack of an accurate $\delta^{18}O_{seawater}$ estimate does not allow for comparison of temperature regimes. Minimums of $\delta^{18}O_{calcite}$ indicate more extreme summer $\delta^{18}O_{calcite}$ in MMCO scallops than MCT. Maximums of $\delta^{18}O_{calcite}$ indicate less extreme winter $\delta^{18}O_{calcite}$ in MMCO scallops then MCT.

Despite a significant difference in $\delta^{18}O_{calcite}$ means (0.21‰) between lighter MMCO and heavier MCT, both intervals recorded summer growth band formation (**Figs. 4.2 & 4.3**). There was less agreement between MMCO annuli and $\delta^{18}O_{calcite}$ than between MCT annuli and $\delta^{18}O_{calcite}$. Oxygen results indicate a much lower longevity and therefore faster growth than suggested by observed annuli (**Table 4.1**).

$\delta^{13}C$ of Chesapecten nefrens. – Carbon isotope analysis of *C. nefrens* contradicted my initial predictions. Productivity was significantly lower in the MMCO interval than that of the MCT interval, and amplitudes of $\delta^{13}C_{calcite}$ MMCO were greater than those of MCT. The lighter mean and wider range of MMCO $\delta^{13}C_{calcite}$ suggests more non-seasonal variability in primary productivity than predicted for the warm interval. The conclusion of a less productive MMCO environment is assuming that difference $\delta^{13}C_{calcite}$ reflected primary productivity. It should be noted that other factors, like thermocline strength and upwelling could also be contributing to the difference in $\delta^{13}C_{calcite}$ between MMCO and MCT. The $\delta^{18}O_{calcite}$ of MCT scallops suggested high

intra-annual variability in physical environmental parameters (i.e. temperature) when compared to the MMCO. However $\delta^{13}C_{calcite}$ of the same MCT scallops suggested primary productivity was relatively stable, and continuous throughout the year when compared to the MMCO (**Fig. 4.4**).

Table 4.1. Comparison of annuli and $\delta^{18}O_{calcite}$ longevities. Annuli of MMCO shells P3 and P7 and MCT shell S5 overestimated isotopic longevity. Annuli of MCT shell S2 accurately estimated isotopic longevity. Annuli at $\delta^{18}O_{calcite}$ lows indicates the number of annuli that coincide with troughs of $\delta^{18}O_{calcite}$.

Shell	**Annuli Age**	**$\delta^{18}O$ Age**	**Annuli at $\delta^{18}O_{calcite}$ lows**
P3	5	3	2
P7	5	3	2
S2	4	4	4
S5	5	3	3

Table 4.2. Stable isotopic data of seasonal extremes. The maximum $\delta^{18}O_{calcite}$ of each annual cycle (Peak) and minimum $\delta^{18}O_{calcite}$ of each annual cycle (Trough). Where a shell had two maximum values, both samples were included. MMCO shells P3 and P7; MCT shells S2 and S5.

Shell	Sample ID	Peak or Trough	Height (mm)	$\delta^{13}C$	$\delta^{18}O$
P3	P3-6	peak 1	19.18	-0.5	0.9
P3	P3-8	peak 1	21.34	-0.5	0.9
P3	P3-33	trough 1	46.97	-0.1	-1.3
P3	P3-43	peak 2	57.69	-0.6	1.4
P3	P3-63	trough 2	81.00	-0.6	-1.3
P3	P3-73	peak 3	91.99	-1.8	1.0
P3	P3-81	trough 3	101.43	-1.7	-0.9
P7	P7_5	peak 1	14.44	0.2	1.1
P7	P7_6	peak 1	15.24	0.3	1.1
P7	P7_33	trough 1	39.06	-0.1	-1.1
P7	P7_60	peak 2	69.28	-0.4	1.2
P7	P7_80	trough 2	92.67	-1.2	-0.8
P7	P7_88	peak 3	101.55	-1.5	1.1
S2	S2-13	trough 1	25.79	-0.1	-1.4
S2	S2-28	peak 1	38.95	-0.3	1.3
S2	S2-58	trough 2	71.14	-0.7	-1.2
S2	S2-66	peak 2	80.24	-0.6	1.2
S2	S2-72	trough 3	86.90	-0.9	-0.3
S2	S2-78	peak 3	92.95	-1.4	1.8
S2	S2-84	trough 4	98.98	-1.1	0.0
S2	S2-87	peak 4	102.00	-1.1	1.7
S5	S5_24	peak 1	41.74	-0.2	1.3
S5	S5_29	peak 1	46.72	-0.1	1.3
S5	S5_63	trough 1	81.71	-0.2	-0.9
S5	S5_79	peak 2	98.27	-0.6	2.0
S5	S5_94	trough 2	114.35	-0.9	-0.9

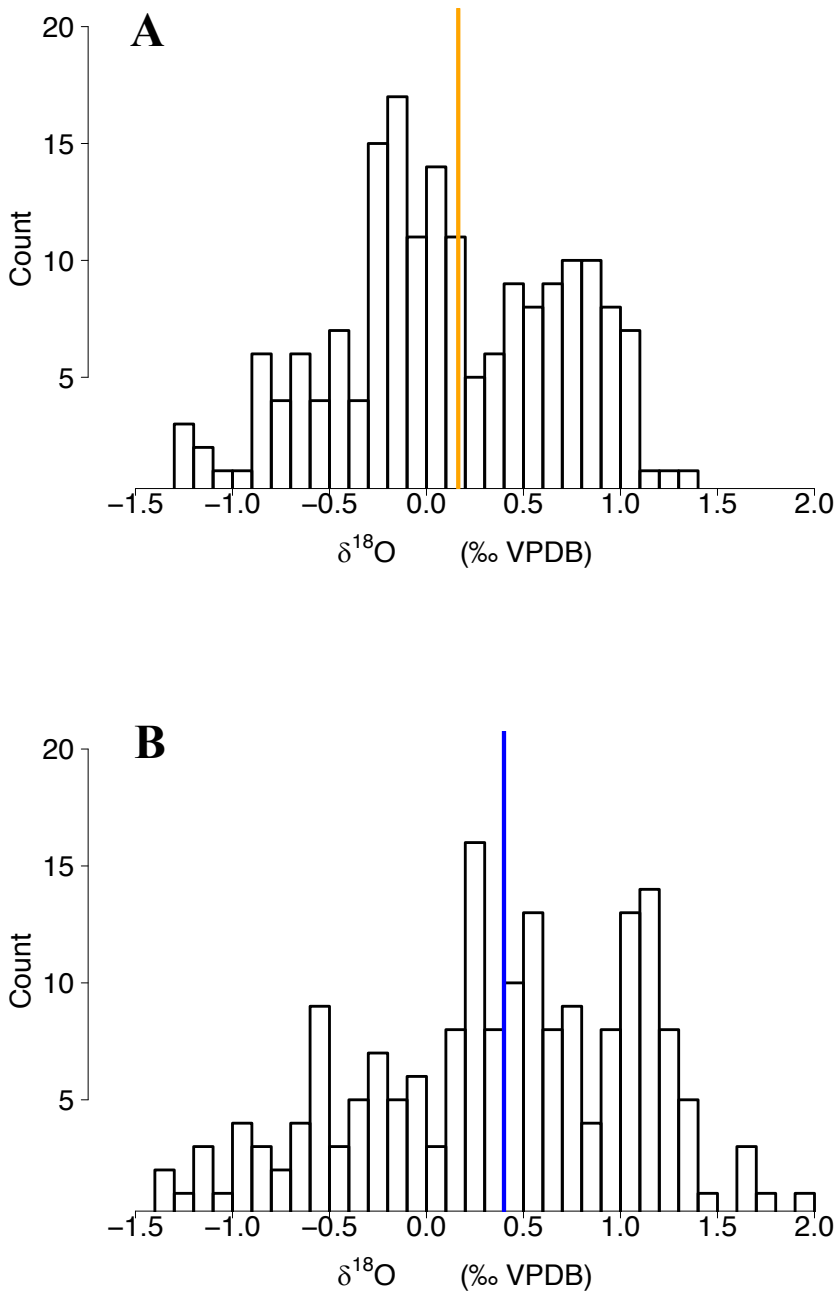

Figure 4.1. Distribution of $\delta^{18}O_{calcite}$ for MMCO and MCT *C. nefrens*. The range of MMCO (**A**.) $\delta^{18}O_{calcite}$ is lesser than MCT (**B**.). Mean MMCO $\delta^{18}O_{calcite}$ (0.16 ‰ VPDB [yellow line, **A**.]) is significantly lighter than mean MCT $\delta^{18}O_{calcite}$ (0.4 ‰ VPDB [blue line, **B**.]; 95% CI of difference in means: -0.37 to -0.10‰).

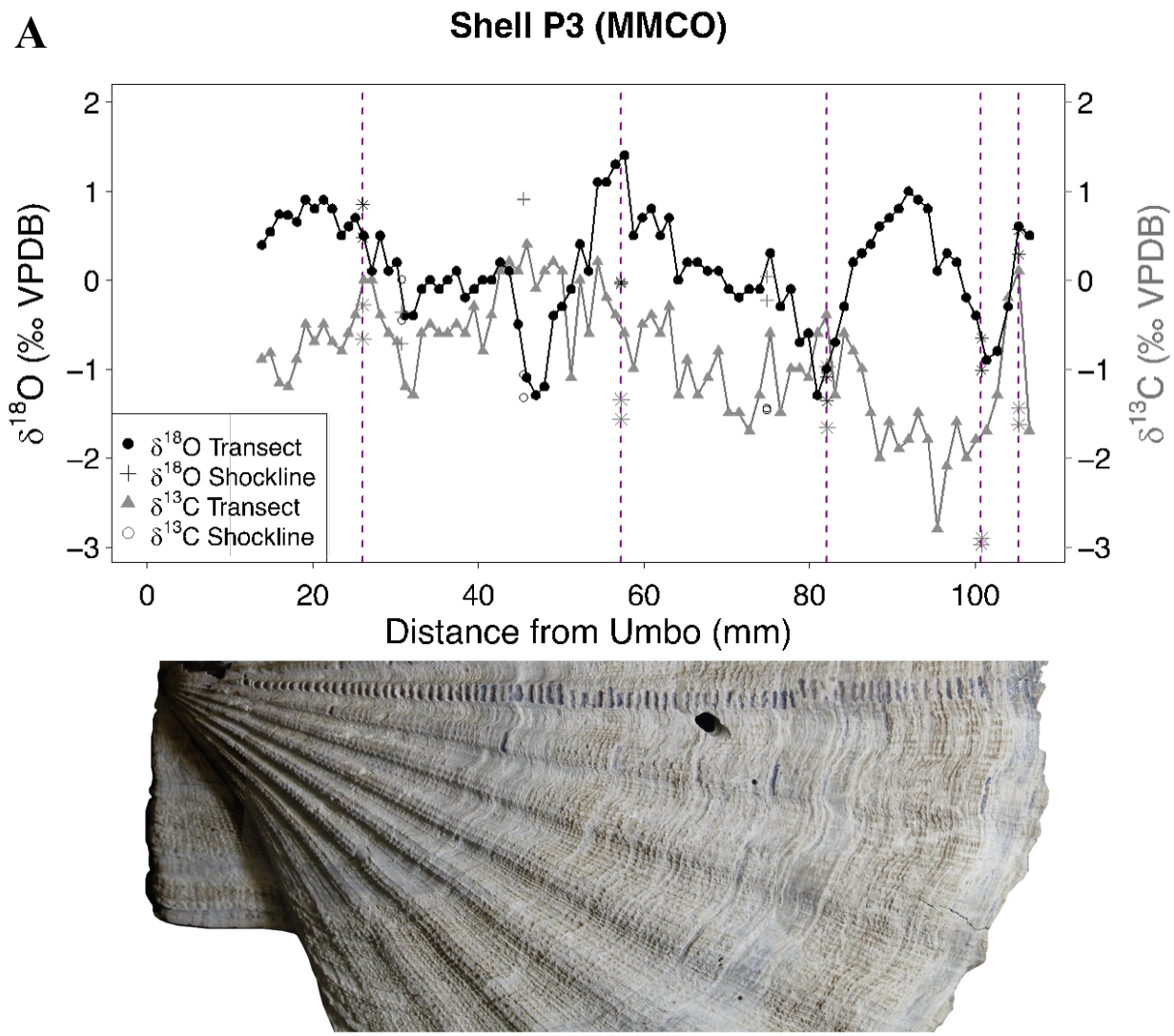

Figure 4.2A. Stable isotopic profile of MMCO *C. nefrens*. (Shell P3) The $\delta^{18}O_{calcite}$ (black dots and line) has seasonal cycles with three troughs around 45 mm, 80 mm and 100 mm. The first trough coincides with an observed shockline (replicate $\delta^{18}O_{calcite}$ shockline is the plus sign). Observed annuli (marked by vertical purple dashed lines) coincide with the second and third $\delta^{18}O_{calcite}$ troughs. Welch one-sample *t*-test of P3 $\delta^{18}O_{calcite}$: mean = 0.15‰ (95% CI: 0.02 to 0.28‰). The $\delta^{13}C_{calcite}$ (grey triangles and line) does not have seasonal cycles. Growth bands do not coincide with $\delta^{13}C_{calcite}$ extremes. A Welch one-sample *t*-test of P3 $\delta^{13}C_{calcite}$: mean=-0.84‰ (95% CI: -0.98 to -0.7‰). P3 stable isotope data in Appendix C: Table C.1.

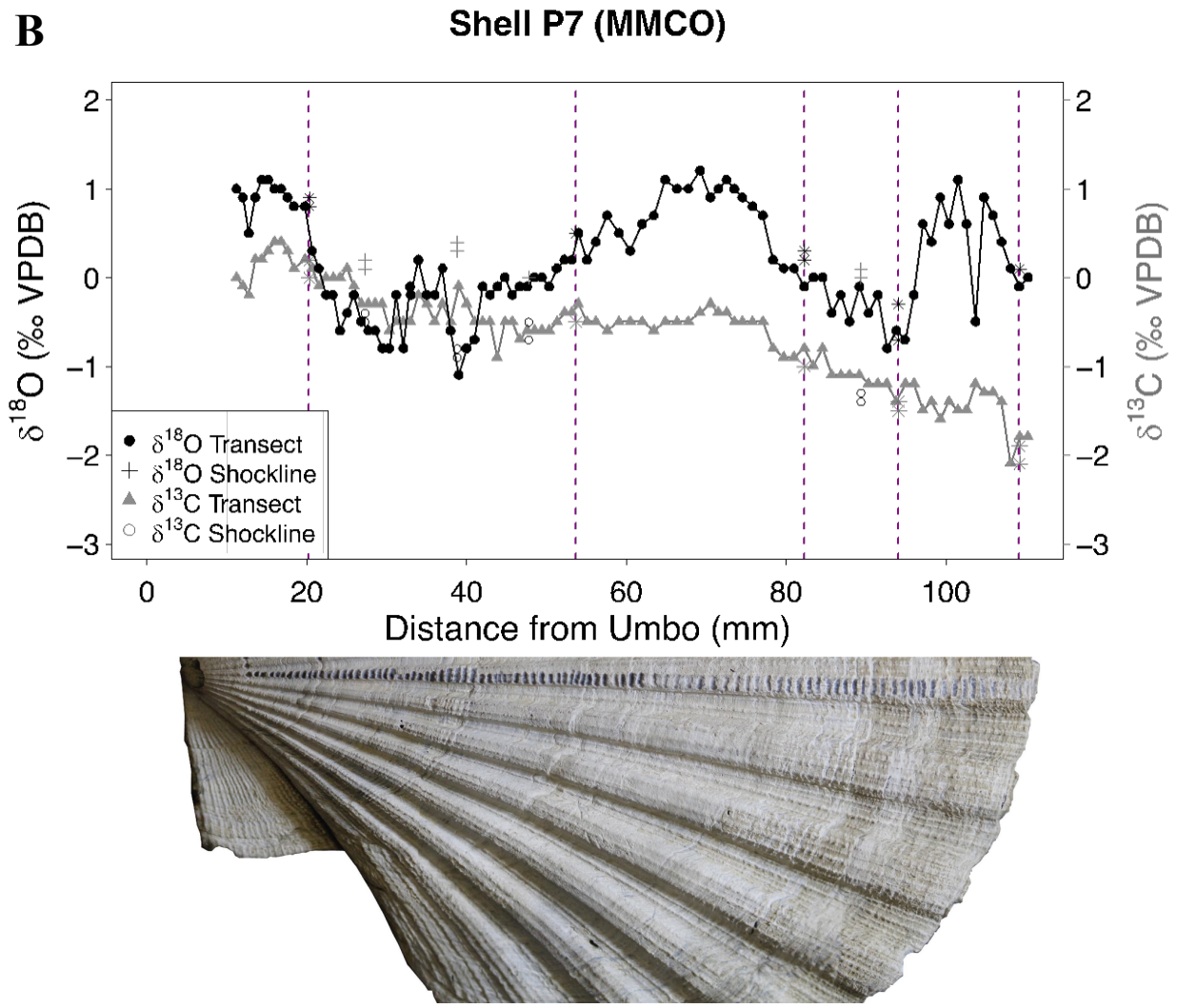

Figure 4.2B. Stable isotopic profile of MMCO *C. nefrens*. (Shell P7) The $\delta^{18}O_{calcite}$ (black dots and line) has seasonal cycles with three troughs around 40 mm, 95 mm and possibly 110 mm. The first trough coincides with an observed shockline (replicate $\delta^{18}O_{calcite}$ shockline is the plus sign). Observed annuli (marked by vertical purple dashed lines) coincide with the second and third $\delta^{18}O_{calcite}$ troughs. Welch one-sample *t*-test of P7 $\delta^{18}O_{calcite}$: mean = 0.18‰ (95% CI: 0.05 to 0.3‰). The $\delta^{13}C_{calcite}$ (grey triangles and line) does not have seasonal cycles. Growth bands do not coincide with $\delta^{13}C_{calcite}$ extremes. A Welch one-sample *t*-test of P7 $\delta^{13}C_{calcite}$: mean=-0.60‰ (95% CI: -0.71 to -0.49‰). P7 stable isotope data in Appendix C: Table C.2.

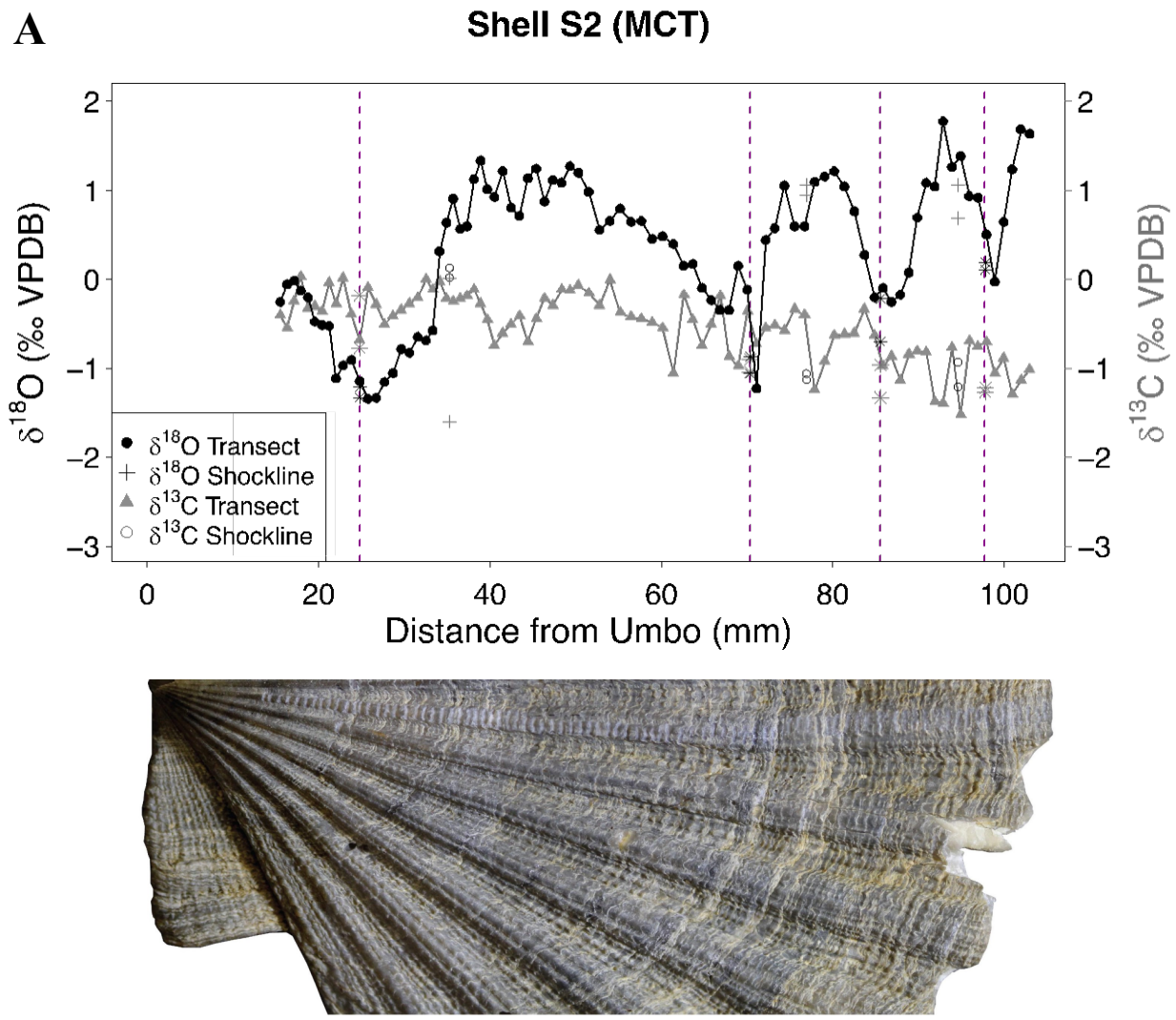

Figure 4.3A. Stable isotopic profile of MCT *C. nefrens*. (Shell S2) The $\delta^{18}O_{calcite}$ (black dots and line) has seasonal cycles with four troughs around 25 mm, 70 mm, 85 mm and 100 mm. Observed annuli (marked by vertical purple dashed lines) coincide with all four $\delta^{18}O_{calcite}$ troughs. Welch one-sample *t*-test of S2 $\delta^{18}O_{calcite}$: mean = 0.34‰ (95% CI: 0.17 to 0.50‰). The $\delta^{13}C_{calcite}$ (grey triangles and line) does not have seasonal cycles. Growth bands do not coincide with $\delta^{13}C_{calcite}$ extremes. A Welch one-sample *t*-test of S2 $\delta^{13}C_{calcite}$: mean=-0.53‰ (95% CI: -0.60 to -0.45‰). S2 stable isotope data in Appendix C: Table C.3.

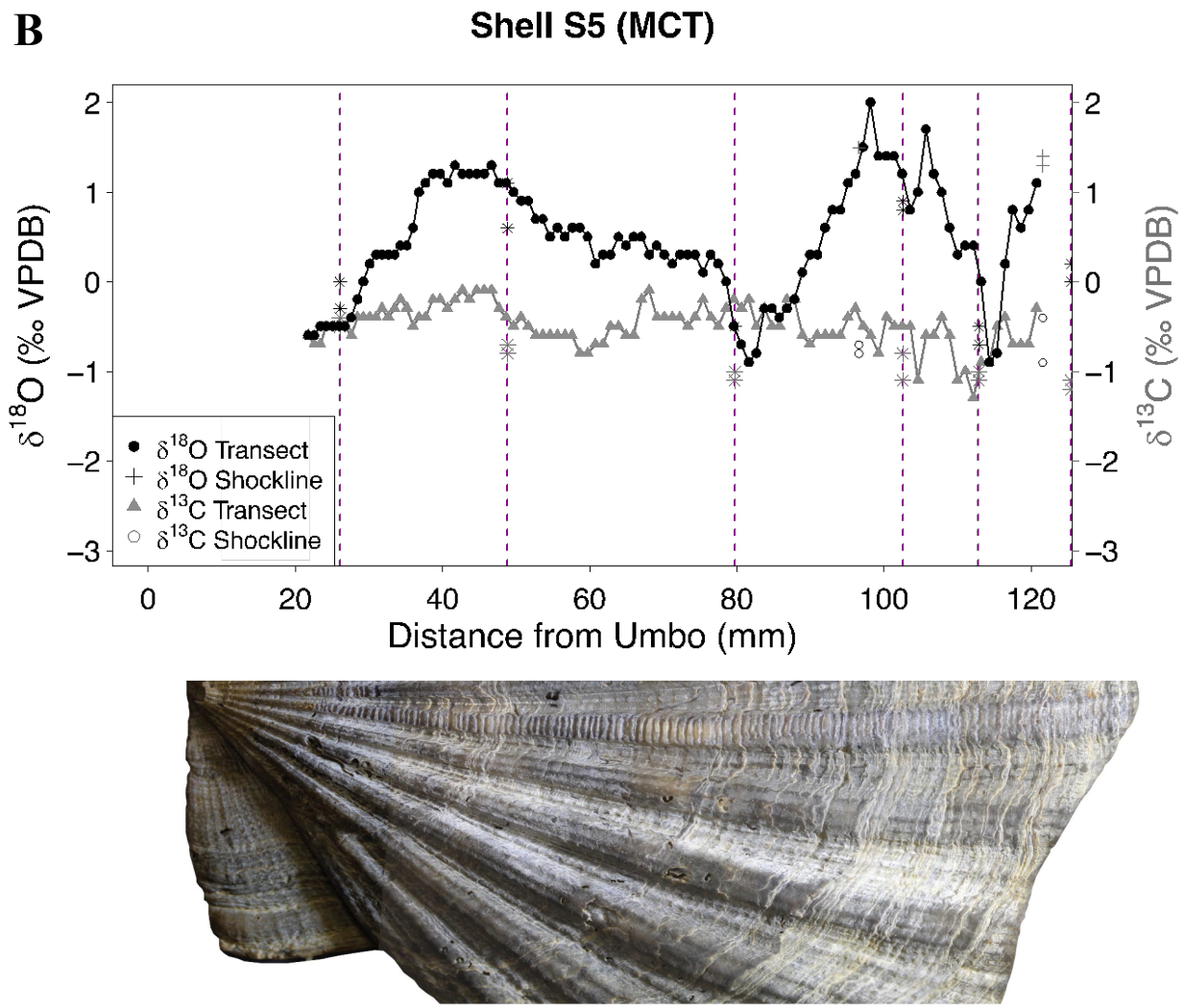

Figure 4.3B. Stable isotopic profile of MCT *C. nefrens*. (Shell S5) The $\delta^{18}O_{calcite}$ (black dots and line) has seasonal cycles with three troughs around 20 mm, 80 mm and 115 mm. Three of the five observed annuli (marked by vertical purple dashed lines) coincide with all three $\delta^{18}O_{calcite}$ troughs. Welch one-sample *t*-test of S5 $\delta^{18}O_{calcite}$: mean = 0.46‰ (95% CI: 0.33 to 0.58‰). The $\delta^{13}C_{calcite}$ (grey triangles and line) does not have seasonal cycles. Growth bands do not coincide with $\delta^{13}C_{calcite}$ extremes. A Welch one-sample *t*-test of S5 $\delta^{13}C_{calcite}$: mean=-0.49‰ (95% CI: -0.53 to -0.44‰). S5 stable isotope data in Appendix C: Table C.4.

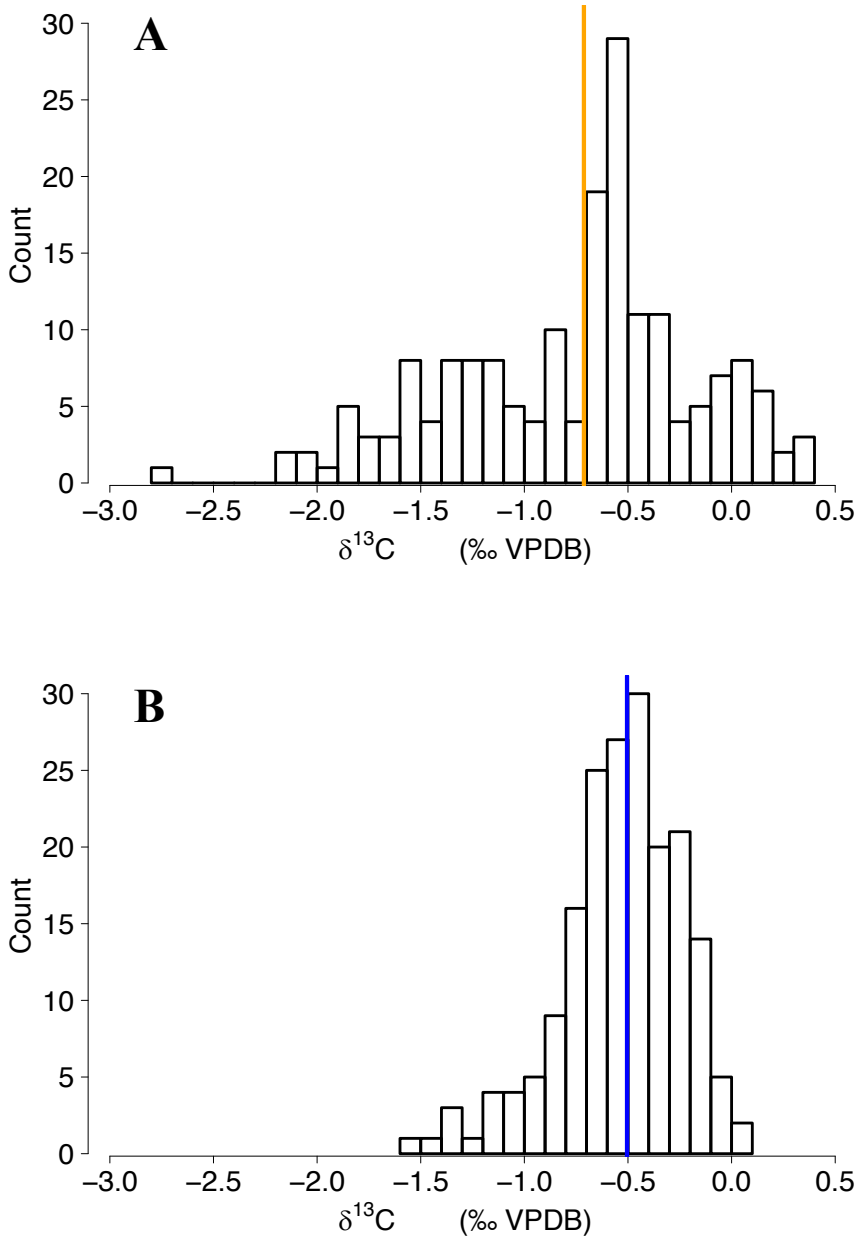

Figure 4.4. Distribution of $\delta^{13}C_{calcite}$ for MMCO and MCT *C. nefrens*. The variance of MMCO (**A.**) $\delta^{13}C_{calcite}$ is significantly different than that of MCT (**B**.) $\delta^{13}C_{calcite}$ (F-test to compare variances: F=4.10, num df=180, denom df=187, p<0.00001). Means, marked by thin lines [**A.** MMCO: orange; **B**. MCT: blue], were significantly lighter in MMCO than MCT $\delta^{13}C_{calcite}$ (Welch two-sample *t*-test: MMCO = –0.71‰ and MCT = -0.50‰ with 95% CI: -0.31 to -0.11‰).

CHAPTER V

GENERAL CONCLUSIONS

At the beginning of the study, seven objectives were provided, three growth related predictions, three stable isotope related predictions, and one final objective. The first prediction was that climate changes in the middle Miocene would instigate lower longevities of MMCO *Chesapecten nefrens* than those of the MCT. The second prediction was that decreasing global temperatures caused a significant decrease in growth rates between MMCO and MCT scallops. The final growth-related prediction was that MMCO scallops would have less abundant shocklines than MCT scallops resulting from less frequent disturbance. The first isotopic prediction was that MMCO $\delta^{18}O$ and $\delta^{13}C$ profiles would have a subdued seasonality when compared to MCT profiles. The second isotope prediction was that mean $\delta^{18}O$ would be lower in MMCO profiles, while $\delta^{13}C$ would be higher in MMCO profiles than MCT. Thirdly, that identified annuli would correspond with peaks or troughs (winter or summer) of isotope profiles. The final objective was to calculate seawater temperature from $\delta^{18}O_{calcite}$.

Longevity and growth determined through identification of annuli did not yield significant differences between the time periods, however annuli overestimated longevity and underestimated growth rate when compared to cycles in oxygen isotopes. Unfortunately, the sample size of $\delta^{18}O_{calcite}$ ages is not great enough to compare $\delta^{18}O_{calcite}$ longevity and growth between MMCO and MCT. Seasonality was present in $\delta^{18}O_{calcite}$ of both the time periods. Seasonal temperature extremes supported hotter MMCO summers than MCT summers, and colder MCT winters than MMCO winters. However, the data supports summer growth cessation

in both MMCO and MCT *C. nefrens*. Middle Miocene climate change was supported by results of isotopic analysis of *C. nefrens*. Both temperatures and productivity varied significantly between the pre-cooling MMCO period and cooled MCT interval. Oxygen isotope cycles reveal that in shallow marine environments, even tropical climates of the MMCO experienced seasonal temperature ranges.

My study supports that scallop growth and stable isotopic compositions provide important insight into paleoenvironments; when considered in combination. Growth and stable isotopic analyses of MMCO and MCT *Chesapecten* have clarified some effects of a rapid climate change on an organism within a single geographic range. Further analysis of *Chesapecten* from shell beds within the Calvert Cliffs has the potential to reveal high-resolution environmental responses to climatic variability through the middle Miocene. With accurate $\delta^{18}O_{seawater}$ estimates for the middle Miocene North Atlantic will allow for changes in seawater temperature to be calculated. With valid seawater temperature calculations, a better estimate of scallop response to the variable Miocene climate will be possible. Further analysis of growth and stable isotopes within *Chesapecten* of the Calvert Cliffs will clarify the effects of Miocene Climate on subtidal environments.

REFERENCES

Billups, K., and Schrag, D.P. 2002. Paleotemperatures and ice volume of the past 27 Myr revisited with paired Mg/Ca and $^{18}O/^{16}O$ measurements on benthic foraminifera. Paleoceanography, 17:1–11.

Bohme, M. 2003. The Miocene Climatic Optimum: evidence from ectothermic vertebrates of Central Europe. Palaeogeography, Palaeoclimatology, Palaeoecology 195:389–401.

Browning, J.V., et al. 2006. Quantification of the effects of eustasy, subsidence, and sediment supply on Miocene sequences, mid-Atlantic margin of the United States. Geological Society of America Bulletin, 118(5/6):567–588.

Chauvaud, L., et al. 1998. Effects of environmental factors on the daily growth rate of *Pecten maximus* juveniles in the Bay of Brest (France). Journal of Experimental Marine Biology and Ecology, 227:83–111

Chauvaud, L., et al. 2005. Shell of the Great Scallop *Pecten maximus* as a high-frequency archive of paleoenvironmental changes. Geochemistry Geophysics Geowsystems, 6:1–15.

Chauvaud, L., J. et al. 2011. What's hiding behind ontogenic $\delta^{13}C$ variations in mollusk shells? New insights from the Great Scallop (*Pecten maximus*). Estuaries and Coasts. 34:211–220.

Chauvaud, L., J. et al. 2012. Variation in Size and Growth of the Great Scallop Pecten maximus along a Latitudinal Gradient PLoS ONE, 7(5):e37717.

Chute, A.S. et al. 2012. Timing of Shell Ring Formation and Patterns of Shell Growth in the Sea Scallop *Placopecten Magellanicus* Based on Stable Oxygen Isotopes. Journal of Shellfish Research, 31(3):649–662.

Diester-Haas, L., et al. 2009. Mid-Miocene paleoproductivity in the Atlantic Ocean and implications for the global carbon cycle. Paleoceanography, 24:PA1209.

Doney, S.C., et al. 2012. Climate impacts on marine ecosystems. Annual Review of Marine Science, 4:11–37.

Emiliani, C. 1966. Isotopic paleotemperatures. Science, 154(3751):851–857.

Flower, B.P., and Kennett, J.P. 1994. Middle Miocene climatic transition: East Antarctic ice sheet development, deep ocean circulation and global cycling. Palaeogeography, Palaeoclimatology, Palaeoecology, 108:537–555.

Goewert, A.E., and D. Surge. 2008. Seasonality and growth patterns using isotope sclerochronology in shells of the Pliocene scallop *Chesapecten madisonius*. Geology and Marine Letters 28:327-338.

Goewert, A.E. 2010. Paleoclimate Archives and Evolutionary Patterns Preserved in Neogene Scallop Shells: Implications for Linking Climate Change, Paleobiogeography, and Morphologic Evolution of Chesapecten along the Atlantic Coastal Plain, USA. PhD thesis, UNC at Chapel Hill, 328 pp.

Greenop, R., Foster, G.L., Wilson, P.A., Lear, C.H. 2014. Middle Miocene climate instability associated with high-amplitude CO_2 variability. Paleoceanography, 29(9):845–853.

Harris, B.P. and K.D.E. Stokesbury. 2006. Shell growth of sea scallops (*Placopecten magellanicus*) in the southern and northern Great South Channel, USA. ICES Journal of Marine Science, 63: 811–821.

Hart, D.R., A.S. Chute. 2009. Verification of Atlantic sea scallop (*Placopecten magellanicus*) shell growth rings by tracking cohorts in fishery closed areas. Canadian Journal of Fisheris and Aquatic Science, 66:751–758.

Hayward, B.W., et al. 2007. Last global extinction in the deep sea during the mid-Pleistocene climate transition. Palaeogeography, Palaeoclimatology, Palaeoecology, 22:1–14

Holburn, A., et al. 2004. Middle Miocene isotope stratigraphy and paleoceanographic evolution of the northwest and southwest Australian margins (Wombat Plateau and Great Australian Bight). Palaeogeography, Palaeoclimatology, Palaeoecology, 208:1–122.

Johnson, A.L.A., et al. 2009. Comparative sclerochronology of modern and mid-Pliocene (c. 3.5 Ma) *Aequipecten opercularis* (Mollusca, Bivalvia): an insight into past and future climate change in the north-east Atlantic region. Palaeogeography, Palaeoclimatology, Palaeoecology, 284: 164–179.

Jones, D.S., and W.D. Allmon. 1995. Records of upwell, seasonality and growth in stable-isotope profiles of Pliocene mollusk shells from Florida. Lethaia, 28:61-74.

Jones, D.S., and S.J. Gould. 1999. Direct Measurement of Age in Fossil *Gryphaea*: The Solution to a Classic Problem in Heterochrony. Paleobiology, 25(2):158–187.

Kidwell, S. 1989. Stratigraphic condensation of marine transgressive records: origin of major shell deposits in the Miocene of Maryland. The Journal of Geology, 97(1):1–24.

Kidwell, S., et al. 2015. Miocene stratigraphy and paleoenvironments of the Calvert Cliffs, Maryland. Geological Society of America: Field Guide, 40:231–279.

Krantz, D.E., D.F. Williams, and D.S. Jones. 1987. Ecological and paleoenvironmental information using stable isotope profiles from living and fossil molluscs. Palaeogeography, Palaeoclimatology, Palaeoecology, 58:249–266.

MacDonald, B.A., R.J. Thmpson. 1988. Intraspecific Variation in Growth and Reproduction in Latitudinally Differentiated Populations of the Giant Scallop Placopecten magellanicus (Gmelin). Biological Bulletin, 175(3):361–371.

Merrill, A.S., J.A. Posgay, and F.E. Nichy. 1961. Annual marks on shell and ligament of Sea scallop (*Placopecten magellanicus*). Fishery Bulletin, 65(2):299–311.

Moss, D.K., et al. 2016. Lifespan, growth rate, and body size across latitude in marine Bivalvia, with implications for Phanerozoic evolution. Proceedings Royal Society B, 283: 20161364.

Owen, R., H. Kennedy, and C. Richardson. 2002. Isotopic partitioning between scallop shell calcite and seawater: Effect of shell growth rate. Geochemica et. Cosmochimica Acta, 66(10):1727–1737.

Ravelo, A.C., C. Hillaire-Marcel. 2007. The Use of Oxygen and Carbon Isotopes of Foraminifera in Paleoceanography. Developments in Marine Geology, Volume 1, Chapter 18:735–764.

Scalfani, J.A. 2011. A Morphological and Phylogenetic Examination of the Miocene and Pliocene Bivalve Genus Chesapecten. Undergraduate Honors Theses. Paper 429.

Schöne, B.R., and D. Surge. 2005. Looking back over skeletal diaries — High-resolution environmental reconstructions from accretionary hard parts of aquatic organisms. Palaeogeography, Palaeoclimatology, Palaeoecology, 228 (1&2):1-3.

Schöne, B.R., and Gillikin, D.P., 2013. Environmental histories from skeletal diaries – Advances in sclerochronology. Palaeogeography, Palaeoclimatology, Palaeoecology, 373:1–5.

De Verteuil, L., and G. Norris. 1996. Miocene Dinoflagellate Stratigraphy and Systematics of Maryland and Virginia. Micropaleontology, 42:i–vii & 1–172.

Vogt, P.R., and M. Parrish. 2012. Driftwood dropstones in Middle Miocene Climate Optimum s hallow marine strata (Calvert Cliffs, Maryland Coastal Plain): Erratic pebbles no certain proxy for cold climate. Palaeogeography, Palaeoclimatology, Palaeoecology, 323–325:100-109.

Waller, T.R. 2006. Phylogeny of families in the Pectinoidea (Mollusca: Bivalvia): importance of the fossil record. Zoological Journal of the Linnean Society, 148:313–342.

Ward, L.W., and B.W. Blackwelder. 1975. *Chesapecten*, a new genus of Pectinidae (Mollusca: Bivalvia) from the Miocene and Pliocene of Eastern North America. Geological Survey Professional Paper.

Zachos J.C., et al. 1993. Climate change and transient climates during the paleogene: A marine perspective. The Journal of Geology 101:191–213.

Zachos, J.C., et al. 2001. Trends, rhythms and aberrations in global climate 65 Ma to present. Science, 292(5517):686–693.

APPENDIX A

Longevity and Growth Data for *C. nefrens*

Table A.1. Longevity and growth of MMCO *C. nefrens*. Total height measured with calipers, number of annuli (individual longevity), and *K* (individual growth) calculated using the von Bertalanffy growth function ($\bar{x}$ *K*= 0.39; 95% CI: 0.32 to 0.47).

Shell Name	Shattuck Bed	Total Height (mm)	Number of Annuli	Number of Shocklines	*K*
C24	14	118.30	5	3	0.44
C25	14	104.08	4	7	0.23
C26	14	115.41	6	3	0.56
C27	14	100.94	5	6	0.25
C28	14	119.64	5	5	0.27
C29	14	118.94	6	3	0.14
C30	14	113.69	7	9	0.53
C31	14	101.53	6	8	0.50
C32	14	110.34	6	8	0.57
M10	14	118.59	4	6	0.41
M11	14	140.80	11	3	0.22
M12	14	130.10	7	6	0.46
M13	14	144.71	8	9	0.38
M14	14	132.38	9	4	0.53
M5	14	102.32	4	8	0.95
M6	14	108.31	5	8	0.23
M7	14	111.13	6	9	0.37
M8	14	117.40	6	7	0.23
M9	14	117.04	5	4	0.25
P1	14	110.11	4	5	0.54
P2	14	111.82	5	3	0.24
P3	14	107.05	4	5	0.09
P4	14	99.89	5	2	0.56
P5	14	98.48	4	4	0.51
P6	14	115.73	4	5	0.41
P7	14	110.32	5	4	0.35

Table A.2. Longevity and growth of MCT *C. nefrens*. Heights measured with calipers, Number of annuli (individual longevity), *K* (individual growth) calculated using the von Bertalanffy growth function ($\bar{x}$ *K*= 0.40; 95% CI: 0.31 to 0.48).

Shell Name	Shattuck Bed	Total Height (mm)	Number of Annuli	Number of Shocklines	*K*
C1	19	142.38	10	4	0.39
C10	19	157.22	8	6	0.25
C11	19	112.26	4	5	0.22
C12	19	99.28	5	5	0.24
C13	19	97.77	4	2	0.55
C14	19	103.95	4	4	0.17
C15	19	99.30	4	3	0.77
C16	19	109.27	5	7	0.28
C17	19	110.81	5	6	0.43
C18	19	104.48	4	2	1.07
C19	19	116.99	7	8	0.49
C2	19	129.67	7	6	0.29
C20	19	106.33	4	5	0.28
C21	19	105.60	5	7	0.73
C22	19	105.23	5	2	0.08
C23	19	103.05	4	6	0.35
C3	19	122.80	7	4	0.40
C4	19	136.18	8	4	0.34
C5	19	133.09	9	4	0.27
C6	19	125.00	8	4	0.37
C7	19	121.74	6	4	0.34
C8	19	124.01	5	3	0.37
C9	19	124.43	7	4	0.42
S1	19	102.97	4	6	0.38
S2	19	102.89	4	5	0.82
S3	19	94.33	4	6	0.41
S4	19	117.95	6	5	0.22
S5	19	138.73	8	6	0.23

Table A.3. Measured annuli heights for each scallop. All annuli identified with their corresponding shell heights for all 54 shells (MMCO n=26 scallops; MCT n=28 scallops). Longevity and growth were calculated using identified annuli and measured heights.

Shell	Annuli	Height (mm)	Bed	Shell	Annuli	Height (mm)	Bed
P7	1	20.58	14	S3	1	20.12	19
P7	2	54.07	14	S3	2	52.22	19
P7	3	80.74	14	S3	3	69.11	19
P7	4	94.93	14	S3	4	82.97	19
P7	5	108.55	14	S3	5	93.31	19
P1	1	17.07	14	S4	1	27.6	19
P1	2	59.52	14	S4	2	52.1	19
P1	3	83.94	14	S4	3	81.25	19
P1	4	98.36	14	S4	4	97.33	19
P2	1	20.93	14	S4	5	111.41	19
P2	2	51.41	14	C11	1	37.89	19
P2	3	73.22	14	C11	2	59.37	19
P2	4	100.31	14	C11	3	80.46	19
P2	5	108.42	14	C11	4	104.6	19
P3	1	25.44	14	C11	5	108.21	19
P3	2	49.7	14	C12	1	27.35	19
P3	3	67.07	14	C12	2	50.34	19
P3	4	82.58	14	C12	3	70.69	19
P3	5	102.28	14	C12	4	83.65	19
P4	1	24.78	14	C12	5	96.17	19
P4	2	57.58	14	C13	1	29.3	19
P4	3	83.47	14	C13	2	62.16	19
P4	4	89.49	14	C13	3	77.92	19
P4	5	98.22	14	C13	4	90.62	19
P5	1	31.61	14	C14	1	31.42	19
P5	2	61.34	14	C14	2	60.72	19
P5	3	76.89	14	C14	3	82.18	19
P5	4	88.73	14	C14	4	103.75	19
P6	1	29.3	14	C15	1	30.75	19
P6	2	66.28	14	C15	2	67.99	19
P6	3	98.72	14	C15	3	78.43	19
P6	4	111.44	14	C15	4	91.17	19
M5	1	31.06	14	C16	1	23.44	19
M5	2	75.76	14	C16	2	53.72	19

M5	3	89.55	14	C16	3	76.38	19
M5	4	99.25	14	C16	4	92.09	19
M6	1	25.38	14	C16	5	106.76	19
M6	2	48.09	14	C17	1	28.91	19
M6	3	78.55	14	C17	2	60.89	19
M6	4	94.39	14	C17	3	80.01	19
M6	5	106.17	14	C17	4	92.38	19
M7	1	28.54	14	C17	5	102.6	19
M7	2	58.13	14	C18	1	34.03	19
M7	3	76.81	14	C18	2	79.78	19
M7	4	92.85	14	C18	3	92.43	19
M7	5	103.92	14	C18	4	100.64	19
M7	6	107.46	14	C19	1	28.19	19
M8	1	24.51	14	C19	2	65.54	19
M8	2	47.45	14	C19	3	83.69	19
M8	3	73.4	14	C19	4	93.65	19
M8	4	84.48	14	C19	5	102.24	19
M8	5	93.83	14	C19	6	108.97	19
M8	6	109.1	14	C19	7	113.16	19
M8	7	115.39	14	C20	1	32.18	19
M9	1	23.58	14	C20	2	58.71	19
M9	2	49.85	14	C20	3	91.89	19
M9	3	72.28	14	C20	4	103.25	19
M9	4	85.15	14	C21	1	41.81	19
M9	5	98.78	14	C21	2	73.72	19
M9	6	109.73	14	C21	3	86.44	19
M10	1	30.99	14	C21	4	93.14	19
M10	2	65.71	14	C21	5	98.95	19
M10	3	92.56	14	C22	1	25.95	19
M10	4	107.8	14	C22	2	44.04	19
M10	5	117.87	14	C22	3	54.76	19
C24	1	35.31	14	C22	4	81.83	19
C24	2	65.24	14	C22	5	93.98	19
C24	3	92.79	14	C22	6	102.83	19
C24	4	107.29	14	C23	1	27.86	19
C24	5	112.13	14	C23	2	61.91	19
C25	1	31.23	14	C23	3	77.6	19
C25	2	58.36	14	C23	4	97.6	19
C25	3	85.92	14	C1	1	25.24	19
C25	4	101.48	14	C1	2	67.4	19

C26	1	35.35	14	C1	3	95.02	19
C26	2	66.71	14	C1	4	101.72	19
C26	3	91.15	14	C1	5	109.87	19
C26	4	99.12	14	C1	6	119.13	19
C26	5	103.62	14	C1	7	126.51	19
C26	6	110.04	14	C1	8	130.53	19
C27	1	22.87	14	C1	9	134.88	19
C27	2	47.83	14	C1	10	139.95	19
C27	3	67.52	14	C2	1	30.18	19
C27	4	86.84	14	C2	2	60.36	19
C27	5	95.31	14	C2	3	78.59	19
C28	1	36.66	14	C2	4	96.43	19
C28	2	61.29	14	C2	5	111.56	19
C28	3	87.94	14	C2	6	117.75	19
C28	4	103.61	14	C2	7	124.57	19
C28	5	114.29	14	C3	1	33.76	19
C29	1	43.6	14	C3	2	65.34	19
C29	2	60.07	14	C3	3	86.64	19
C29	3	78.67	14	C3	4	99.58	19
C29	4	93.2	14	C3	5	106.99	19
C29	5	108.29	14	C3	6	114.07	19
C29	6	115.03	14	C3	7	121.09	19
C30	1	33.13	14	C4	1	34.93	19
C30	2	66.16	14	C4	2	59.48	19
C30	3	87.74	14	C4	3	91.23	19
C30	4	98.81	14	C4	4	102.77	19
C30	5	103.73	14	C4	5	111.02	19
C30	6	108.24	14	C4	6	119	19
C30	7	113.18	14	C4	7	126.5	19
C31	1	28.76	14	C4	8	130.88	19
C31	2	58.76	14	C5	1	23.22	19
C31	3	79.9	14	C5	2	49.75	19
C31	4	89.79	14	C5	3	74.1	19
C31	5	96.68	14	C5	4	90.69	19
C31	6	101.12	14	C5	5	103.56	19
C32	1	32.59	14	C5	6	111.05	19
C32	2	70.2	14	C5	7	120.21	19
C32	3	81.33	14	C5	8	126.95	19
C32	4	93.02	14	C5	9	129.87	19
C32	5	100.21	14	C6	1	38.19	19

C32	6	105.57	14	C6	2	64.74	19
M11	1	23.68	14	C6	3	87.35	19
M11	2	54.42	14	C6	4	99.85	19
M11	3	75.61	14	C6	5	109.32	19
M11	4	89.71	14	C6	6	117.5	19
M11	5	95.67	14	C6	7	120.77	19
M11	6	101.57	14	C6	8	122.7	19
M11	7	105.82	14	C7	1	32.4	19
M11	8	119.14	14	C7	2	61.01	19
M11	9	127.34	14	C7	3	83.13	19
M11	10	131.33	14	C7	4	100.42	19
M11	11	136.52	14	C7	5	110.55	19
M12	1	31.18	14	C7	6	116.74	19
M12	2	68.59	14	C8	1	24.77	19
M12	3	93.98	14	C8	2	57.9	19
M12	4	104.3	14	C8	3	86.66	19
M12	5	119.62	14	C8	4	102.51	19
M12	6	123.53	14	C8	5	113.43	19
M12	7	126.45	14	C9	1	30.44	19
M13	1	35.9	14	C9	2	60.67	19
M13	2	71.44	14	C9	3	88.79	19
M13	3	101.92	14	C9	4	101.23	19
M13	4	112.46	14	C9	5	110.49	19
M13	5	120.91	14	C9	6	116.91	19
M13	6	131.95	14	C9	7	120.68	19
M13	7	138.66	14	C10	1	40.98	19
M13	8	143.92	14	C10	2	72.72	19
M14	1	25.72	14	C10	3	92.54	19
M14	2	66.5	14	C10	4	108.78	19
M14	3	99.15	14	C10	5	137.26	19
M14	4	109.23	14	C10	6	145.22	19
M14	5	117.5	14	C10	7	150.02	19
M14	6	121.61	14	C10	8	154.34	19
M14	7	125.52	14	S5	1	25.24	19
M14	8	129.73	14	S5	2	48.71	19
M14	9	132.1	14	S5	3	79.62	19
S1	1	25.73	19	S5	4	95.97	19
S1	2	61.96	19	S5	5	103.57	19
S1	3	85.34	19	S5	6	113.2	19
S1	4	102.68	19	S5	7	125.89	19

S2	1	25.45	19	S5	8	136.87	19
S2	2	71.03	19				
S2	3	85.66	19				
S2	4	98.65	19				

APPENDIX B

Shell Calcite XRD Data for *C. nefrens*

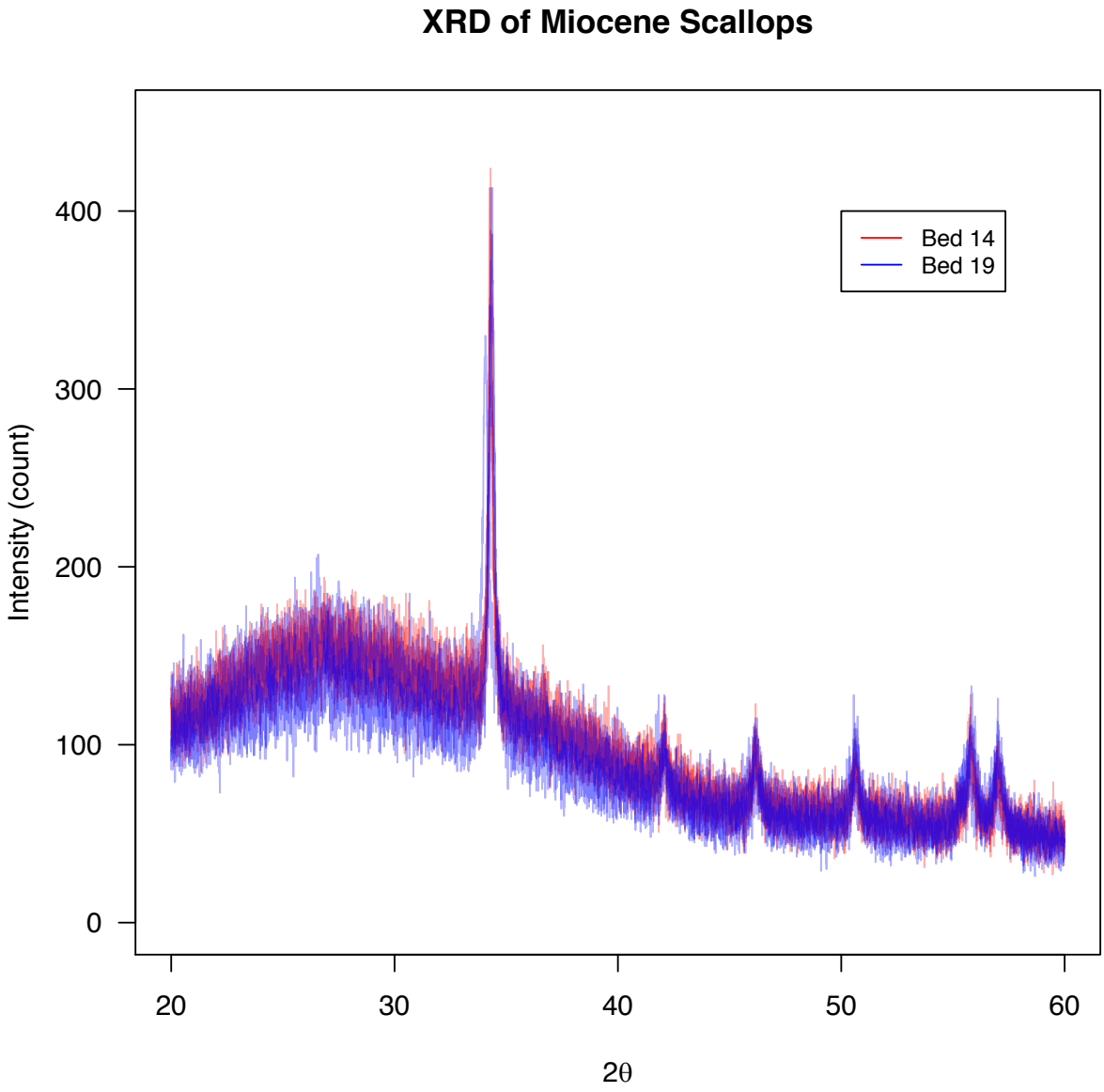

Figure B.1. XRD results of MMCO and MCT shell calcite. The small samples size resulted in a gradual hump at ~25 which was an overprint from the amorphous glass slide. XRD results indicate that all *C. nefrens* were calcite.

APPENDIX C

Isotopic Data for *C. nefrens* ($\delta^{18}O_{calcite}$ and $\delta^{13}C_{calcite}$)

Table C.1. Oxygen and Carbon stable isotope data for MMCO shell P3 (height 107.05 mm). Distance from umbo measured along axis of growth.

Sample Name	Distance from umbo (mm)	$\delta^{13}C_{calcite}$ (‰)	$\delta^{18}O_{calcite}$ (‰)
P3-1	13.87	-0.89	0.39
P3-2	14.93	-0.82	0.54
P3-3	15.99	-1.16	0.74
P3-4	17.06	-1.21	0.73
P3-5	18.12	-0.89	0.65
P3-6	19.18	-0.5	0.9
P3-7	20.26	-0.7	0.8
P3-8	21.34	-0.5	0.9
P3-9	22.42	-0.7	0.8
P3-10	23.50	-0.8	0.5
P3-11	24.36	-0.6	0.6
P3-12	25.22	-0.4	0.7
P3-13	26.22	0	0.5
P3-14	27.21	0	0.1
P3-15	28.21	-0.4	0.5
P3-16	29.20	-0.6	0.1
P3-17	30.20	-0.7	0.2
P3-18	31.19	-1.2	-0.4
P3-19	32.19	-1.3	-0.4
P3-20	33.18	-0.6	-0.1
P3-21	34.24	-0.5	0
P3-22	35.30	-0.6	-0.1
P3-23	36.36	-0.6	0
P3-24	37.42	-0.5	0.1
P3-25	38.48	-0.6	-0.2
P3-26	39.53	-0.3	-0.1
P3-27	40.59	-0.8	0
P3-28	41.65	-0.4	0

P3-29	42.71	0.1	0.2
P3-30	43.77	0.2	0.1
P3-31	44.84	0.1	-0.5
P3-32	45.90	0.4	-1.1
P3-33	46.97	-0.1	-1.3
P3-34	48.04	0.1	-1.2
P3-35	49.11	0.2	-0.4
P3-36	50.17	0.1	-0.3
P3-37	51.24	-1.1	-0.1
P3-38	52.31	0	0.4
P3-39	53.37	-0.6	0.1
P3-40	54.44	0.2	1.1
P3-41	55.52	-0.2	1.1
P3-42	56.61	-0.4	1.3
P3-43	57.69	-0.6	1.4
P3-44	58.77	-1	0.5
P3-45	59.86	-0.5	0.7
P3-46	60.94	-0.4	0.8
P3-47	62.02	-0.6	0.5
P3-48	63.10	-0.3	0.7
P3-49	64.19	-1.3	0
P3-50	65.27	-0.9	0.2
P3-51	66.52	-1.3	0.2
P3-52	67.77	-1.1	0.1
P3-53	69.03	-0.8	0.1
P3-54	70.28	-1.5	-0.1
P3-55	71.53	-1.5	-0.2
P3-56	72.78	-1.7	-0.1
P3-57	74.03	-1.3	-0.1
P3-58	75.29	-0.6	0.3
P3-59	76.54	-1.5	-0.3
P3-60	77.79	-1	-0.1
P3-61	78.86	-1	-0.7
P3-62	79.93	-1.1	-0.6
P3-63	81.00	-0.6	-1.3
P3-64	82.07	-0.4	-1
P3-65	83.15	-1.3	-0.7
P3-66	84.22	-0.6	-0.3
P3-67	85.29	-0.8	0.2
P3-68	86.36	-1	0.3

P3-69	87.43	-1.5	0.4
P3-70	88.50	-2	0.6
P3-71	89.66	-1.6	0.7
P3-72	90.83	-1.9	0.8
P3-73	91.99	-1.8	1
P3-74	93.16	-1.5	0.9
P3-75	94.32	-1.8	0.8
P3-76	95.48	-2.8	0.1
P3-77	96.65	-2.1	0.3
P3-78	97.81	-1.6	0.2
P3-79	98.98	-2	-0.2
P3-80	100.14	-1.8	-0.4
P3-81	101.43	-1.7	-0.9
P3-82	102.72	-1.3	-0.8
P3-83	104.02	-0.2	-0.3
P3-84	105.31	0.1	0.6
P3-85	106.60	-1.7	0.5

Table C.2. Oxygen and Carbon stable isotope data for MMCO shell P7 (height 110.32 mm). Distance from umbo measured along axis of growth.

Sample Name	Distance from umbo (mm)	$\delta^{13}C_{calcite}$ (‰)	$\delta^{18}O_{calcite}$ (‰)
P7_1	11.24	0	1
P7_2	12.04	-0.1	0.9
P7_3	12.84	-0.2	0.5
P7_4	13.64	0.2	0.9
P7_5	14.44	0.2	1.1
P7_6	15.24	0.3	1.1
P7_7	16.04	0.4	1
P7_8	16.84	0.4	1
P7_9	17.64	0.3	0.9
P7_10	18.44	0.1	0.8
P7_11	19.82	0.2	0.8
P7_12	20.70	0.1	0.3
P7_13	21.58	-0.1	0.1
P7_14	22.46	0	-0.2
P7_15	23.34	0	-0.2
P7_16	24.22	0	-0.6
P7_17	25.10	0.1	-0.4
P7_18	25.98	-0.1	-0.2
P7_19	26.86	-0.3	-0.5
P7_20	27.74	-0.3	-0.6
P7_21	28.62	-0.3	-0.6
P7_22	29.50	-0.3	-0.8
P7_23	30.38	-0.6	-0.8
P7_24	31.26	-0.5	-0.2
P7_25	32.14	-0.5	-0.8
P7_26	33.02	-0.5	-0.1
P7_27	33.06	-0.5	-0.2
P7_28	34.06	-0.2	0.2
P7_29	35.06	-0.3	-0.2
P7_30	36.06	-0.5	-0.2
P7_31	37.06	-0.3	0.1
P7_32	38.06	-0.5	-0.6
P7_33	39.06	-0.1	-1.1
P7_34	40.06	-0.3	-0.8
P7_35	41.06	-0.5	-0.7

P7_36	42.06	-0.5	-0.1
P7_37	42.99	-0.5	-0.2
P7_38	43.92	-0.9	-0.1
P7_39	44.85	-0.5	0
P7_40	45.78	-0.5	-0.2
P7_41	46.71	-0.7	-0.1
P7_42	47.64	-0.6	-0.1
P7_43	48.57	-0.6	0
P7_44	49.50	-0.6	0
P7_45	50.43	-0.6	-0.1
P7_46	51.36	-0.5	0.1
P7_47	52.29	-0.4	0.2
P7_48	53.22	-0.4	0.2
P7_49	54.06	-0.3	0.5
P7_50	55.15	-0.5	0.2
P7_51	56.23	-0.5	0.4
P7_52	57.68	-0.6	0.7
P7_53	59.13	-0.5	0.5
P7_54	60.58	-0.5	0.3
P7_55	62.03	-0.5	0.6
P7_56	63.48	-0.6	0.7
P7_57	64.93	-0.5	1.1
P7_58	66.38	-0.5	1
P7_59	67.83	-0.5	1
P7_60	69.28	-0.4	1.2
P7_61	70.59	-0.3	0.9
P7_62	71.59	-0.4	1
P7_63	72.59	-0.4	1.1
P7_64	73.59	-0.5	1
P7_65	74.55	-0.5	0.9
P7_66	75.85	-0.5	0.8
P7_67	77.15	-0.5	0.7
P7_68	78.45	-0.8	0.2
P7_69	79.75	-0.9	0.1
P7_70	81.05	-0.9	0.1
P7_71	82.33	-0.8	-0.1
P7_72	83.47	-1	0
P7_73	84.61	-0.8	0
P7_74	85.75	-1.1	-0.4
P7_75	86.89	-1.1	-0.2

P7_76	88.03	-1.1	-0.5
P7_77	89.22	-1.1	-0.1
P7_78	90.37	-1.2	-0.4
P7_79	91.52	-1.2	-0.2
P7_80	92.67	-1.2	-0.8
P7_81	93.85	-1.4	-0.6
P7_82	94.95	-1.2	-0.7
P7_83	96.05	-1.2	-0.2
P7_84	97.15	-1.5	0.6
P7_85	98.25	-1.4	0.4
P7_86	99.35	-1.6	0.9
P7_87	100.45	-1.4	0.6
P7_88	101.55	-1.5	1.1
P7_89	102.65	-1.5	0.6
P7_90	103.75	-1.2	-0.5
P7_91	104.85	-1.3	0.9
P7_92	105.95	-1.3	0.7
P7_93	107.05	-1.4	0.4
P7_94	108.15	-2.1	0.1
P7_95	109.25	-1.8	-0.1
P7_96	110.32	-1.8	0

Table C.3. Oxygen and Carbon stable-isotope data for MCT shell S2 (height 102.89 mm). Distance from umbo measured along axis of growth.

Sample Name	Distance from umbo (mm)	$\delta^{13}C_{calcite}$ (‰)	$\delta^{18}O_{calcite}$ (‰)
S2-1	15.56	-0.41	-0.26
S2-2	16.37	-0.55	-0.06
S2-3	17.19	-0.25	-0.02
S2-4	18.00	0.03	-0.13
S2-5	18.82	-0.33	-0.21
S2-6	19.63	-0.31	-0.48
S2-7	20.45	-0.37	-0.52
S2-8	21.26	-0.04	-0.53
S2-9	22.08	-0.28	-1.12
S2-10	22.89	0.01	-0.97
S2-11	23.86	-0.4	-0.91
S2-12	24.83	-0.69	-1.15
S2-13	25.79	-0.1	-1.35
S2-14	26.76	-0.29	-1.34
S2-15	27.73	-0.51	-1.16
S2-16	28.70	-0.42	-1.06
S2-17	29.67	-0.35	-0.79
S2-18	30.63	-0.28	-0.83
S2-19	31.60	-0.21	-0.65
S2-20	32.57	0	-0.69
S2-21	33.37	-0.12	-0.58
S2-22	34.17	-0.03	0.31
S2-23	34.96	-0.22	0.63
S2-24	35.76	-0.25	0.9
S2-25	36.56	-0.22	0.56
S2-26	37.36	-0.19	0.59
S2-27	38.16	-0.12	1.12
S2-28	38.95	-0.28	1.33
S2-29	39.75	-0.46	1.01
S2-30	40.55	-0.75	0.92
S2-31	41.53	-0.61	1.21
S2-32	42.51	-0.51	0.8
S2-33	43.49	-0.42	0.71
S2-34	44.47	-0.71	1.13
S2-35	45.45	-0.45	1.24
S2-36	46.43	-0.22	0.87

S2-37	47.41	-0.3	1.11
S2-38	48.39	-0.12	1.08
S2-39	49.37	-0.13	1.27
S2-40	50.35	-0.07	1.19
S2-41	51.58	-0.16	0.98
S2-42	52.81	-0.3	0.55
S2-43	54.04	-0.01	0.65
S2-44	55.27	-0.38	0.79
S2-45	56.51	-0.43	0.64
S2-46	57.74	-0.45	0.65
S2-47	58.97	-0.49	0.45
S2-48	60.20	-0.55	0.48
S2-49	61.43	-1.06	0.39
S2-50	62.66	-0.18	0.15
S2-51	63.72	-0.46	0.17
S2-52	64.78	-0.75	-0.1
S2-53	65.84	-0.51	-0.24
S2-54	66.90	-0.19	-0.35
S2-55	67.96	-0.87	-0.35
S2-56	69.02	-0.98	0.15
S2-57	70.08	-0.36	-0.12
S2-58	71.14	-0.73	-1.23
S2-59	72.20	-0.55	0.44
S2-60	73.26	-0.52	0.57
S2-61	74.42	-0.58	1.05
S2-62	75.59	-0.34	0.59
S2-63	76.75	-0.41	0.59
S2-64	77.91	-1.25	1.09
S2-65	79.08	-0.93	1.15
S2-66	80.24	-0.64	1.21
S2-67	81.40	-0.62	1.04
S2-68	82.56	-0.61	0.76
S2-69	83.73	-0.34	0.27
S2-70	84.89	-0.64	-0.21
S2-71	85.90	-0.98	-0.1
S2-72	86.90	-0.87	-0.26
S2-73	87.91	-1.14	-0.18
S2-74	88.92	-0.85	0.07
S2-75	89.93	-0.81	0.69
S2-76	90.93	-0.82	1.08

S2-77	91.94	-1.38	1.04
S2-78	92.95	-1.4	1.77
S2-79	93.95	-0.77	1.26
S2-80	94.96	-1.53	1.38
S2-81	95.97	-0.7	0.93
S2-82	96.97	-0.76	0.91
S2-83	97.98	-0.71	0.5
S2-84	98.98	-1.06	-0.03
S2-85	99.99	-0.89	0.64
S2-86	100.99	-1.3	1.23
S2-87	102.00	-1.14	1.68
S2-88	103.00	-1.02	1.63

Table C.4. Oxygen and Carbon stable-isotope data for MCT shell S5 (height 138.73 mm). Distance from umbo measured along axis of growth.

Sample Name	Distance from umbo (mm)	$\delta^{13}C_{calcite}$ (‰)	$\delta^{18}O_{calcite}$ (‰)
S5_1	21.77	-0.6	-0.6
S5_2	22.61	-0.7	-0.6
S5_3	23.45	-0.7	-0.5
S5_4	24.29	-0.5	-0.5
S5_5	25.13	-0.5	-0.5
S5_6	25.97	-0.5	-0.5
S5_7	26.81	-0.5	-0.5
S5_8	27.65	-0.6	-0.4
S5_9	28.49	-0.4	-0.2
S5_10	29.33	-0.4	0
S5_11	30.17	-0.4	0.2
S5_12	31.01	-0.4	0.3
S5_13	31.85	-0.3	0.3
S5_14	32.69	-0.4	0.3
S5_15	33.53	-0.3	0.3
S5_16	34.37	-0.2	0.4
S5_17	35.21	-0.3	0.4
S5_18	36.05	-0.5	0.6
S5_19	36.89	-0.4	1
S5_20	37.75	-0.4	1.1
S5_21	38.75	-0.2	1.2
S5_22	39.74	-0.2	1.2
S5_23	40.74	-0.3	1.1
S5_24	41.74	-0.2	1.3
S5_25	42.74	-0.1	1.2
S5_26	43.73	-0.2	1.2
S5_27	44.73	-0.1	1.2
S5_28	45.73	-0.1	1.2
S5_29	46.72	-0.1	1.3
S5_30	47.72	-0.3	1.1
S5_31	48.72	-0.4	1.1
S5_32	49.71	-0.5	1
S5_33	50.71	-0.4	0.9
S5_34	51.71	-0.5	0.9
S5_35	52.71	-0.6	0.7
S5_36	53.70	-0.6	0.7

S5_37	54.70	-0.6	0.5
S5_38	55.70	-0.6	0.6
S5_39	56.69	-0.6	0.5
S5_40	57.69	-0.6	0.6
S5_41	58.74	-0.8	0.6
S5_42	59.78	-0.8	0.5
S5_43	60.83	-0.7	0.2
S5_44	61.87	-0.7	0.3
S5_45	62.92	-0.5	0.3
S5_46	63.96	-0.5	0.5
S5_47	65.01	-0.6	0.4
S5_48	66.05	-0.6	0.5
S5_49	67.10	-0.2	0.5
S5_50	68.15	-0.1	0.3
S5_51	69.19	-0.4	0.4
S5_52	70.24	-0.4	0.3
S5_53	71.28	-0.4	0.2
S5_54	72.33	-0.4	0.3
S5_55	73.37	-0.5	0.3
S5_56	74.42	-0.4	0.3
S5_57	75.46	-0.2	0.1
S5_58	76.51	-0.4	0.3
S5_59	77.55	-0.5	0.2
S5_60	78.60	-0.3	0
S5_61	79.64	-0.2	-0.5
S5_62	80.67	-0.3	-0.7
S5_63	81.71	-0.2	-0.9
S5_64	82.74	-0.5	-0.8
S5_65	83.78	-0.3	-0.3
S5_66	84.81	-0.5	-0.3
S5_67	85.85	-0.5	-0.4
S5_68	86.88	-0.2	-0.3
S5_69	87.92	-0.2	-0.2
S5_70	88.95	-0.6	0.1
S5_71	89.99	-0.7	0.3
S5_72	91.02	-0.6	0.3
S5_73	92.06	-0.6	0.6
S5_74	93.09	-0.6	0.8
S5_75	94.13	-0.6	0.8
S5_76	95.16	-0.4	1.1

S5_77	96.20	-0.3	1.2
S5_78	97.23	-0.5	1.5
S5_79	98.27	-0.6	2
S5_80	99.30	-0.8	1.4
S5_81	100.38	-0.4	1.4
S5_82	101.45	-0.5	1.4
S5_83	102.53	-0.5	1.2
S5_84	103.60	-0.5	0.8
S5_85	104.68	-1.1	1
S5_86	105.75	-0.6	1.7
S5_87	106.83	-0.6	1.2
S5_88	107.90	-0.4	1
S5_89	108.98	-0.6	0.6
S5_90	110.05	-1.1	0.3
S5_91	111.13	-1	0.4
S5_92	112.20	-1.3	0.4
S5_93	113.28	-0.9	0
S5_94	114.35	-0.9	-0.9
S5_95	115.43	-0.5	-0.8
S5_96	116.50	-0.4	0.2
S5_97	117.58	-0.7	0.8
S5_98	118.65	-0.7	0.6
S5_99	119.73	-0.7	0.8
S5_100	120.80	-0.3	1.1